Virtual Reconstruction of Pelvic Fractures

by

Maha Samir Ali Ead

A thesis submitted in partial fulfillment of the requirements for the degree of

Master of Science

Department of Mechanical Engineering

University of Alberta

Abstract

Pelvic fractures are severe injuries that are associated with high rates of mortality and morbidity, especially in the elderly population. In severe cases of fracture, urgent surgical intervention may be required with the use of fixation plates to stabilize the fracture. The surgical planning process of these fractures is complicated and time consuming, which could potentially increase the risk on the patients. Therefore, this thesis aims to provide a method for virtually reconstructing fractured pelvises with the goal of easing the surgical planning process and improving surgical outcomes.

For unilaterally fractured pelvises, pelvic symmetry was examined first to conclude whether the contralateral side can be used as a template for rebuilding the fractured side. Pelvic bilateral symmetry was evaluated by studying intact pelvises and calculating the differences between the left and right sides with the use of 3D deviation analyses. Results showed that the pelvis exhibits remarkable left-right symmetry, confirming that the uninjured sides of fractured pelvises can serve as viable models in virtual pelvis reduction. A reconstruction technique is presented and assessed in this thesis. It is a semi-automatic method that can provide accurate virtual reconstructions with deviations within the clinically acceptable range for preventing osteoarthritis in the hip joints.

For bilaterally fractured pelvises, there is no intact model to serve as a template for the reconstruction procedure. Therefore, average pelvic shape models were developed to work as templates for the reconstruction. Separate average shape models were developed for male and female hemipelves to account for sex differences in pelvic shape. Statistical shape modeling was used to build these average shape models from a group of intact pelvises. Differences in shape

between the average shape models and the respective intact pelvises from which they were developed is discussed in this thesis. The average shape models were then used as templates to reconstruct unilaterally fractured pelvises. The results were compared to the same pelvises that were reconstructed by using the opposite intact sides as templates, in order to evaluate the quality of the reduction. Finally, the method for reconstructing bilaterally fractured pelvises using the average shape template is presented.

Developing an accurate virtual reconstruction method for different types of pelvic fracture has the potential to lower the overwhelmingly high mortality and morbidity rates. Surgeons will be able to provide better treatments for these patients by offering quicker treatment proposals and easing the design process of the fixation plates for surgery. This can reduce the wait times for patients prior to surgery while preserving the quality of the planned reconstruction procedure.

Preface

This thesis is an original work by Maha Ead. The research project required the use of CT scan images of the pelvic region. Therefore, ethics approval was received from the University of Alberta Research Ethics Board, Project Name "Investigating pelvic geometry for the study of optimized fracture fixation", No. Pro00092224, July 5, 2019.

Chapter 3 of this thesis has been published as Ead MS, Duke KK, Jaremko JL, Westover L (2020) Investigation of pelvic symmetry using CAD software. Med Biol Eng Comput 58:75–82. https://doi.org/10.1007/s11517-019-02068-w. I was responsible for conducting the research, analyzing the results and writing the manuscript. Dr. Jaremko, assisted in analyzing the results from a medical perspective and reviewing the manuscript. Dr. Duke and Dr. Westover were the supervisory authors. They assisted in developing the methodology, analyzing the results and editing the manuscript.

Chapter 4 of this thesis has been published as Ead MS, Westover L, Polege S, McClelland S, Jaremko JL, Duke KK (2020) Virtual reconstruction of unilateral pelvic fractures by using pelvic symmetry. Int J Comput Assist Radiol Surg 15:1267–1277. https://doi.org/10.1007/s11548-020-02140-z. I was responsible for the data collection, analysis and manuscript composition. Polege and McClelland assisted in obtaining the results by applying our methods. Dr. Jaremko, assisted in the analysis and review of the manuscript. Dr. Westover and Dr. Duke were the supervisory authors and were involved with concept formation, analysis and manuscript edits.

Acknowledgements

First and foremost, I would like to express my utmost gratitude to God, the Almighty, for giving me the strength and determination to complete this thesis successfully. This work would not have been possible without His countless blessings.

I am thankful to my supervisors, Dr. Lindsey Westover and Dr. Kajsa Duke for their endless support and guidance. Their knowledge and expertise in the area was essential for the completion of this work. I am forever grateful for their encouragement, patience and advice both academically and personally. They have become my mentors and friends over the past two years and I have learned a great deal from them.

I would also like to acknowledge the support of the Natural Sciences and Engineering Research Council of Canada (NSERC) for funding this research work.

I am incredibly grateful for the love and support of my family and friends. I would like to thank my sister and brother for believing in me and always being there to help me get through the difficult times. Finally, I would like to extend my deepest appreciation to my parents for their understanding and encouragement throughout this stressful time. Their constant support, motivation and prayers was all I needed.

Table of Contents

List of Tables

List of Figures

Chapter 1: Introduction

1.1 Background and Motivation

The human pelvic bone has an irregular morphological shape which makes it prone to serious fractures when injured. In some complex cases, the bone may be shattered into several fragments and involve damage to the surrounding soft tissue. As a result of this, pelvic fractures are associated with the highest rates of mortality and morbidity in musculoskeletal injuries [1]. The mortality rate for patients with complex fractures accompanied with soft tissue injuries exceeds 33% [2, 3]. These mortality and morbidity rates run even higher for elderly patients over the age of 60 [4, 5].

Patients with pelvic fractures need urgent treatment with surgical intervention and the use of pelvic clips, metal plates or screws [6, 7]. Their surgical treatment plans involve collaboration between various healthcare professionals and requires many hospital resources, which may be limited at the time [8]. This could potentially delay the treatment process and increase the risk on the patient. In addition, some severe cases of pelvic injury require customized components to be manufactured for stabilizing the fracture which can delay surgery by 4-6 weeks [9].

Pelvic fractures are known to be one of the most difficult injuries to treat, due to associated complications, as well as limited surgical access to the intricate areas of the pelvis [10]. Not to mention, the strict criteria that must be adhered to in order to limit or prevent post-operative osteoarthritis in the hip joints [11–16]. Studies have shown that accurate preoperative planning are necessary for a successful reconstruction or reduction of the pelvis [17, 18].

Virtual pelvic fracture reconstruction methods have been introduced to assist in the surgical planning process. These methods are successful in reducing operation times and providing good reductions, but they have limitations [11]. In these methods, the user manually moves the fractured pieces to the proper location. Therefore, they can only be performed by expert medical professionals, which makes them subjective, as well as time consuming. For these reasons, this thesis aims to provide a solution for the current limitations in handling pelvic fractures. This will be accomplished by proposing a relatively quick and semi-automatic method for building accurate 3D virtual models of reduced pelvises that orthopedic surgeons can use as templates for planning their surgeries and developing custom fracture fixation plates. Our method provides accurate

reconstructions while minimizing user-subjectivity and only requires basic computer software skills.

1.2 Objectives

The main objective of this research is to develop a method for virtual pelvic fracture reconstruction of both unilaterally and bilaterally fractured pelvises. This will assist surgeons by providing them with a 3D reference model of a reduced pelvis for the surgical planning procedure. The specific aims (SA) of this project are listed below.

SA 1: For unilateral fractures, pelvic symmetry will be investigated first to conclude that the contralateral side can be used as a template for reconstructing the fractured side.

SA 2: Virtual reconstruction for unilateral fractures will be developed by mirroring the uninjured hemipelvis and using it to align the fracture pieces.

SA 3: For the bilateral fractured pelvises, average male and female left and right hemipelvis shapes will be created from a group of intact adult pelvises and then used to serve as templates for the reconstruction. The average hemipelvis shapes will be scaled to the same volume as the fractured pelvises, in order to account for size variations. Finally, the fractured pieces will be aligned with the average hemipelvis shape to form a model of a reconstructed pelvis.

1.3 Thesis Outline

The research conducted in this thesis is presented as follows:

Chapter 1 provides a brief introduction to the topic by describing the motivation behind the work. It also includes a list of research objectives which provide a viable solution to the issue at stake.

Chapter 2 provides the necessary background as well as a review of the literature in the area.

Chapter 3 presents the research conducted on the left-right symmetry of the pelvis. The methods used to study this symmetry are introduced and the results are presented using both qualitative and quantitative data. A conclusion about pelvic symmetry is then made.

Chapter 4 presents a method for virtually reconstructing pelvises that are broken on one side by using the opposite intact side as a template. The quality of the reduced hemipelves is evaluated by comparing them to their intact sides. Results include quantitative statistics and color maps.

Chapter 5 presents the average pelvic shapes developed for both males and females. The reduction quality is evaluated by reconstructing the unilaterally fractured pelvises introduced in Chapter 4 using the average pelvic shapes as templates and comparing these results with those presented in Chapter 4. The method used to reconstruct bilaterally fractured pelvises is also presented and evaluated.

Chapter 6 includes a conclusion of this thesis and presents recommendations for work that can be implemented in the future.

Chapter 2: Literature Review

2.1 Pelvis Anatomy

Anatomical directions are used to describe the location of different elements in the human body. The terms used in this research and their equivalent definition in lay terms are: anterior (front), posterior (back), superior (above), inferior (below), medial (towards the middle) and lateral (towards the edge).

The hip or pelvis serves as a weight-bearing structure and is the connection point between the upper body and each of the lower limbs. It is made up of two innominate bones that are linked to the skeleton posteriorly at the sacrum, (lower end of the vertebral column). These two hip bones (or coxal bones), the left and right sides of the pelvis, are also joined together anteriorly through the pubic symphysis [19, 20]. The entire structure, including the hip bones, sacrum and coccyx forms the pelvis (Fig. 2.1).

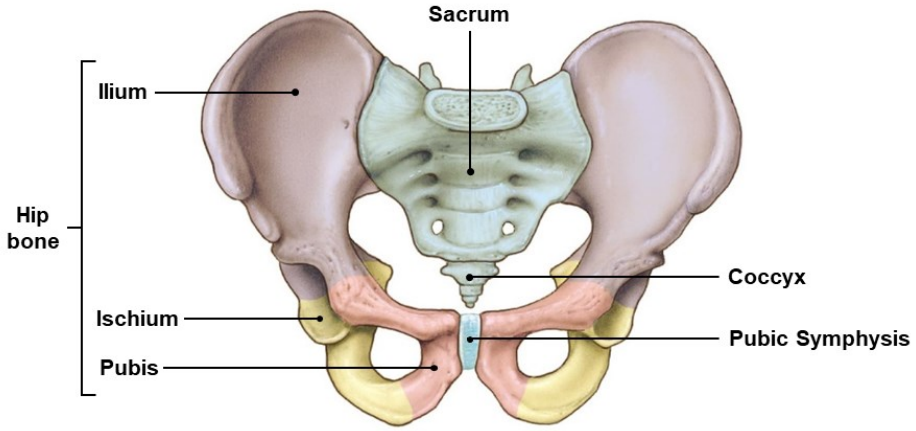

Fig. 2.1 The pelvis connects the lower limbs to the skeleton through the sacrum. It is the made up of the hip bones, sacrum and coccyx. The adult hip bone is made up of three main regions, the ilium, ischium and pubis (adapted from: https://www.thinglink.com/scene/866024238958510081).

The hip bone is the focal point of this research. It is made up of three separate bones, the ilium, ischium and pubis, which merge together throughout teenage years to form one bone (Fig. 2.1). The same names are used to define the different regions of an adult hip bone. The ilium forms the largest section of the hip bone; it has a wing-like structure and connects to the sacrum through the sacroiliac joint. The ischium is the posteroinferior section of the hip bone and gives support to the

body whilst sitting. The pubis is the anteromedial section of the hip bone and connects to the opposite pubis through the pubic symphysis joint as shown in Fig. 2.1. These three regions join in the center to form the acetabulum, a cup-shaped cavity, which is part of the hip joint [19].

2.2 Pelvis Coordinate System

It is important to note that identifying a proper local coordinate system is essential for referring to specific regions of the pelvis. One of the most commonly used coordinate systems for the pelvis is that developed by Cappozzo et al. [21]. They identified the three principal planes by using anatomical landmarks. The origin was first defined as the midpoint between the right and left anterior superior iliac spines (RASIS and LASIS). The z axis is the line passing through the RASIS and LASIS, with its positive direction towards the RASIS. The x axis is the line passing through the midpoint between the right and left posterior superior iliac spines (RPSIS and LPSIS) and the origin, with its positive direction from back to front. The xz plane defines the quasi-transverse plane. The y axis is orthogonal to this quasi-transverse plane, with its positive direction upwards. Finally, the xy plane defines the quasi-sagittal plane and the yz plane defines the quasi-coronal plane [21]. Fig. 2.2 shows the position of the anatomical landmarks used to define this coordinate system, as well as the three planes. This coordinate system was used throughout this thesis, however, for simplicity, the three planes are referred to as the axial plane (quasi-transverse plane), sagittal plane (quasi-sagittal plane) and coronal plane (quasi-coronal plane).

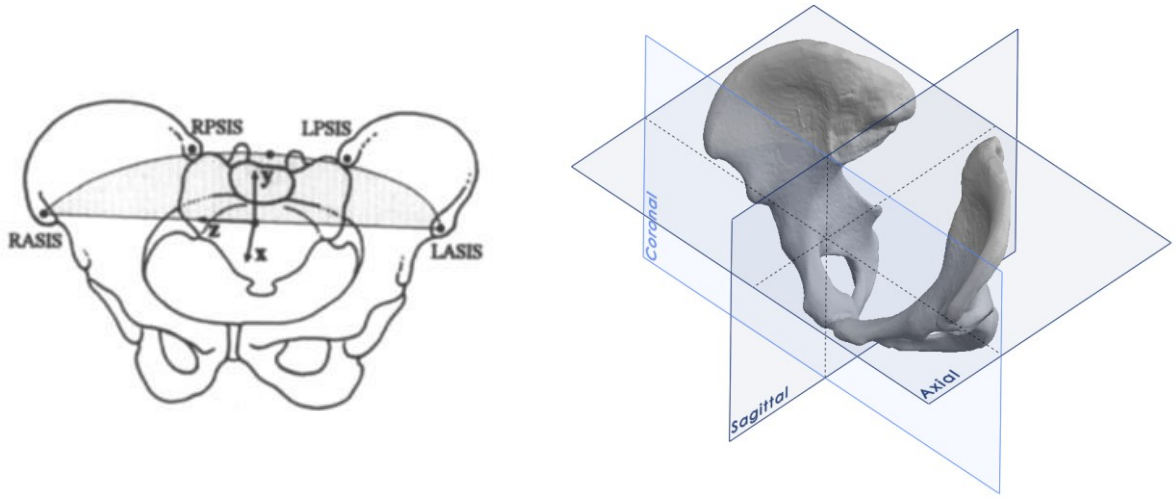

(a) (b)

Fig. 2.2 (a) The pelvis local coordinate system, as defined by Cappozzo et al. The anatomical landmarks used to define this coordinate system are labelled, as well as the origin and local axes [21]. (b) The three local planes.

2.3 Pelvic Fracture Classification

Pelvic fractures occur when large forces with high kinetic energy impact the body at the pelvic region. These incidents mostly result from motor vehicle accidents or falls from great heights [22]. To better understand the significance of pelvic fractures, it is important to discuss the classification systems used. A well-established classification system enables healthcare professionals to properly communicate with their patients and propose suitable treatments [22]. It should minimize intra- and inter-observer subjectivity, include all the possible scenarios and be mutually exclusive, so each fracture falls into one category only [23].

The Letournel and Judet classification [16] is one of the earliest to be established and it categorizes pelvic fractures based on their location. This includes fracture sites, such as the acetabulum, posterior ring and anterior ring [16]. Pennal et al. [24] developed another classification system that distinguishes fractures by the direction of the force that causes the injury. The three main directions of force in this classification are anteroposterior compression (APC), lateral compression (LC) and vertical shear (VS) [24]. Later, Tile et al. [23] modified Pennal's classification to include pelvic stability and treatments. In his model, a stable fracture would be categorized as type A, where there is no instability in the pelvic ring. A type B fracture is a partially stable one, where it is stable vertically and posteriorly, but unstable rotationally. Finally, type C is a completely unstable fracture, where the pelvic ring is unstable rotationally and vertically [23]. These unstable fractures generally require surgical intervention and are often associated with other injuries to the surrounding soft tissue [22].

Another classification that was also modified from Pennal's is the Young and Burgess [25]. It is the most commonly used classification system, since it allows surgeons to implement appropriate treatment protocols quickly [26]. This classification includes the magnitude of forces applied and has an additional category for combined mechanical loads (CM) [25]. Table 2.1 summarizes the different categories of the Young and Burgess classification and their distinguishing factors.

Table 2.1 The Young and Burgess classification system [25].

Category	Fracture Site	Differentiating Characteristic
LC-I	Anterior transverse (pubic rami)	Sacral compression on side of impact
LC-II		Iliac wing fracture
LC-III		Contralateral open-book (APC) injury
APC-I	Symphyseal diastasis or anterior vertical	Slight widening of pubic symphysis and/or sacroiliac joint; stretched but intact anterior and posterior ligaments
APC-II		Widened sacroiliac joint; disrupted anterior ligaments; intact posterior ligaments
APC-III		Complete hemipelvis separation, but no vertical displacement; complete sacroiliac joint disruption; complete anterior and posterior ligament disruption
VS	Symphyseal diastasis or anterior vertical	Vertical displacement anteriorly and posteriorly, usually through sacroiliac joint, occasionally through iliac wing and/or sacrum
CM	Anterior and/or posterior, vertical and/or transverse components	Combination of other injury patterns: LC/VS or LC/APC

2.4 Bilateral Symmetry

Symmetry is a geometric property which implies that two structures have the same shape, but different orientation [27]. Bilateral symmetry is one specific type of symmetry which indicates that two opposite objects are mirror images of each other; they are the same object when reflected across a distinct plane. Rotoinversion symmetry is another type of symmetry that describes objects which require reflection and rotation. Finally, translational symmetry involves both reflection and translation in order for objects to match their counterparts [28].

Human bilateral symmetry has proven useful in many biomedical engineering and clinical applications. When one side of the body is injured, the contralateral healthy side can be utilized to make deductions and plan operations to restore the affected side to its original shape. Bilateral symmetry of the skeleton is used to estimate skeletal age [29]. This can be helpful in forensic research, when only one side of the skeleton is available for evaluation. In orthopedics, bilateral symmetry has been used to develop models of the uninjured bones, which can serve as patient-specific templates in the surgical planning process [30]. This method has been applied to develop customized implants for the talus bone in the human ankle joint [31–33].

In some severe pelvic fracture cases, customized plates are required for securing the pelvis in the correct shape. In current surgical procedures, these customized plates are produced by using

standard straight plates and bending them into shape during the surgery, which prolongs the operation time [34]. Creating virtual 3D models of reconstructed pelvises could allow for these custom plates to be designed and manufactured prior to surgery. For unilaterally fractured pelvises, the 3D models can be created by using the contralateral side as a template for the reconstruction process. However, in order to do so, pelvic symmetry would need to be examined first and evaluated.

Previous studies have used different methods for evaluating pelvic symmetry. Boulay et al. studied 71 anatomical landmarks on either side of 12 pelvis specimens and reported 56 of these landmarks to be symmetric [35]. Osterhoff et al. also analyzed left-right symmetry of the periacetabular surface of the pelvis. They used a pre-shaped acetabular implant to measure the distances between it and 516 pelvis models. Results showed that the periacetabular region of the pelvis is considered symmetric [36]. However, the methods presented in these studies are limited to specific points or regions of the pelvis; and do not quantify symmetry of the entire 3D geometrical surface.

Therefore, in this research, the symmetry of the 3D pelvic surface will be investigated to determine whether the contralateral intact side can be used as a template for rebuilding the fractured side. Ultimately, these reconstructed pelvises can be used as models for shaping the custom fixation plates for surgery.

2.5 Virtual Pelvis Reduction

Computer-aided surgery (CAS) is becoming more popular in clinical applications where health care professionals and technicians use computer-aided design (CAD) software to improve surgical outcomes [37]. It has limitless applications in various fields, such as craniofacial, orthopedic and orthodontic surgeries [38–40]. Three-dimensional computer models are used in the surgical planning processes and have proven to enhance the results of these surgeries [37, 39, 40].

As previously discussed, the pelvis has a complex morphological shape. Additionally, there is limited surgical access to areas such as the hip joints [11]. Therefore, fractures in the pelvis, particularly the acetabular region, are challenging procedures for orthopedic surgeons to handle. For these reasons, CAS has been established for pelvic fracture reconstruction surgeries to assist in preoperative planning [11].

Previous studies have developed techniques and planning tools for virtually reconstructing fractured pelvises. Computerized tomography (CT) scans of the fractured pelvises are first converted into 3D models using image processing software. The pelvises are then reassembled into the appropriate shape by manually placing the fractured pelvic pieces in their correct location. Finally, the fixation plates are virtually contoured over the reduced pelvis and can be manufactured prior to surgery [10, 41–45]. Another study followed the same procedure of developing virtual 3D models from CT scans, however, they utilized the bilaterally symmetric nature of the pelvis to reflect the intact hemipelvis across the sagittal plane and 3D print it. The physical model was then used as template for shaping the fixation plates [46].

Although, these virtual pelvis reconstruction techniques reduce operation times by eliminating the need to bend the fixation plates during the surgery, they also have limitations. The former method requires manual reconstruction, thus it is subjective and user-dependent. Not to mention, it is time consuming and must be performed by an expert medical professional in the field. Additionally, the reconstruction does not utilize the patient's intact hemipelvis as a template but instead relies on the user's expertise, which may affect the reduction quality. The latter reconstruction method also has a constraint of not being able to identify the exact locations of the fractures on the intact hemipelvis model, which could lead to inaccurate contouring of the fixation plates. Furthermore, 3D printing a 1:1 scale model of a hemipelvis takes nearly 24 hours [46], which delays the surgery and increases the wait times for patients.

In this research, a new virtual pelvis reconstruction technique is introduced to overcome the weaknesses of current methods. For the unilaterally fractured pelvises, bilateral symmetry will be used, which will preserve the natural geometrical shape. The method is not reliant on the availability of a medical professional since it only requires basic computer skills. In addition, the reconstruction semi-automatic, which limits user subjectivity and reduces time.

2.6 Statistical Shape Models in Orthopedics

Statistical shape models (SSM) describe the variations in shape within a population by providing an average shape model. They are generated by using a dataset of bones and supplying the model with an expected initial shape from which to build this average shape. Naturally, a larger dataset would provide a better SSM that is representative of all shape variations in the population. These

models can be built in 2D or 3D, depending on the application and the type of imaging available. Three-dimensional SSM are generally created from CT or MRI images that are first converted into 3D models [47].

There are many applications for SSM in orthopedics, such as osteoarthritis (OA) detection [47]. OA normally begins with a degeneration of the protective cartilage covering the bone ends at the joints. However, changes in bone shape are also considered to be a factor that could lead to OA [48]. Diagnosis of OA can be radiographic or clinical, based on reported patient pain experience. Health professionals monitor the progression and development of OA by measuring geometric properties in the radiographic images. However, complicated bone shapes, cannot be fully described using these geometric measures [47]. Therefore, researchers have begun using SSM for accurately quantifying shape deformations, in order to assess OA progression [49]. They also compared differences in shape between healthy subjects and those with OA. By doing so, they were able to identify individuals who are more likely to develop OA [49].

SSM has also proven quite useful in the field of orthopedic implant design. Orthopedic implants go through a rigorous design process and require many tests before confirming their reliability for clinical use. Despite this, these implants may fail to perform up to the desired standard, because of variations in bone shape within the population. SSM could be used to design appropriately shaped implants by analyzing the morphological shape variations between individuals [47]. These models can then be converted into finite element (FE) models for testing. The optimal implant shape with the desired mechanical properties can then be determined [50, 51].

Another application of SSM is in preoperative surgical planning. The benefits of implementing virtual pelvis reconstruction prior to surgery has been previously discussed in Section 2.5. This has encouraged researchers to establish protocols for the treatment of different cases of pelvic fracture [52]. Bilaterally fractured pelvises do not have a viable intact side to serve as a template in the reconstruction procedure, as with unilaterally fractured pelvises. Therefore, in this thesis, average shapes for the male and female left and right hemipelves are developed with SSM to be used in the virtual reconstruction of bilaterally fractured pelvises. These average shapes are developed for the hemipelvis, rather than the entire structure of the pelvis, which includes the sacrum. Since this work focuses on fractures in the hip bone, it is important to capture the morphological shape of that bone in itself.

2.7 Summary

The above review summarizes the current methods of evaluating pelvic symmetry and the available virtual reconstruction techniques for unilaterally fractured pelvises. This thesis aims to overcome the limitations of the current techniques and expand virtual reconstruction to include bilaterally fractured pelvises. In the following chapters pelvic symmetry is evaluated and a novel technique for virtual pelvic fracture reconstruction is introduced. Also, the use of SSM in building an average pelvic shape model is discussed and used to reconstruct bilaterally fractured pelvises.

Chapter 3: Pelvis Symmetry

This chapter was published in the Medical & Biological Engineering & Computing journal:

Ead MS, Duke KK, Jaremko JL, Westover L (2020) Investigation of pelvic symmetry using CAD software. Med Biol Eng Comput 58:75–82. https://doi.org/10.1007/s11517-019-02068-w

3.1 Abstract

Severe pelvic fractures often prove difficult for surgeons as they require patient-specific surgical treatment plans and customized equipment. Developing virtual patient-specific 3D pelvis models would ease the surgical planning process and enable development of custom fixation plates. This paper aims to examine pelvic symmetry to conclude whether the contralateral side may be used as a reference model for the fractured side of the pelvis. Fourteen subjects with intact pelvises were involved in this study. CT scans of the pelvises were converted to 3D models and the right sides of the pelvises were reflected and aligned with the left sides. A deviation analysis was then performed for each set of models and results showed that the average root mean square (RMS) of values was 1.14 ± 0.26 mm and the average percentage of points below a deviation threshold of ± 2 mm was 91.9 ± 5.55%. The deviation color maps (DCMs) showed that the largest deviations were on the non-articular surfaces. The volume and surface area of each model were also examined and showed no significant differences between left and right sides. These results indicate that the pelvis displays bilateral symmetry and this concept can be used to develop fully intact patient-specific 3D pelvis models for fracture reconstruction using the unfractured contralateral side.

3.2 Introduction

The concept of human bilateral symmetry has been introduced to assist in various clinical and biomedical engineering applications. The term bilateral symmetry in this context implies that one part of a body is a mirror image of the opposite side when reflected about a unique plane. An application where human bilateral symmetry has proved important is in estimating skeletal age [29]. In some cases, only one side of the body is viable for evaluation, therefore, knowing that the skeleton is symmetric would ensure that correct deductions are being made when using that one side [29]. Bilateral symmetry has also been used to study the impact of facial symmetry on attractiveness [53]. Another application is to evaluate the effect of atherosclerosis on the left and

right carotid arteries to determine whether one could be used to infer information about the opposite one [54]. Tümer et al. also studied bilateral symmetry of the bones forming the talocrural joint and subtalar joints in the human ankle to investigate whether the contralateral limb may be used as a template in clinical practice and research [30]. The idea of bilateral symmetry has also proven useful in orbital reconstruction surgeries where the unaffected side is virtually reflected and superimposed on the deformed orbit to define the defect; a customized patient-specific implant is then manufactured [55].

The human pelvic bone has an irregular shape and as a result of this, fractures resulting from injuries are often quite complex. In these cases, the bone may be shattered into multiple small pieces, with significantly high rates of mortality and even higher rates of morbidity [1]. Due to associated injuries, patients with complex pelvic fractures have a mortality rate which exceeds 33% [6]. Patients require urgent treatment especially in cases where the pelvic fracture is accompanied by soft tissue injuries and hemodynamic instability [6]. However, due to limited access to resources and the complexity of the fractures [8], patients may have to endure delayed treatment as a result of the time taken in analyzing their specific cases. Improperly treated complex pelvic fractures can lead to lifelong morbidity.

Treatments of pelvic fractures may require surgical intervention and the use of screws and/or metal plates [7, 56] to secure the pelvis in the correct shape and orientation. However, in some cases, where the bone is shattered due to severe fractures, customized plates need to be designed for the patients [9]. During pelvic fracture surgeries, these fixation plates are bent into the desired shape during the operation, which significantly prolongs the operation time [34]. To address this limitation, custom plates could be designed and manufactured prior to surgery through surgical planning with computer-aided design (CAD) technology. The use of CAD software in preoperative planning has been introduced in many surgeries, including mandibular and orbital reconstructions [55, 57, 58]. Not only does this technique improve the overall surgical outcomes, but also reduces costs and operation times [55, 57, 58].

One way to assist with the design of pelvic fixation plates is to develop patient-specific 3D models of their pelvises. A similar approach for ankle fractures quantified the left-right symmetry of the talus bone, confirming that the contralateral talus could be used as a patient-specific 3D model for the injured talus [27]. Symmetry of human orbital walls has also been investigated in order to

confirm the use of the mirroring tool in orbital reconstruction surgeries [59]. Analogous to this, we could design patient-specific 3D models for pelvic fracture repair if pelvic symmetry could be confirmed. Previous studies have exploited different methods of evaluating symmetry of various regions of the pelvis. They used anatomical landmarks to compare bilateral asymmetry [35] or studied the difference between sample pelvises with reference to pre-shaped implants [36]. Not only are these methods subject to significant intra- and inter-observer reliability, but these studies also failed to evaluate symmetry using the entire 3D geometry of the pelvis, in other words, all points of all regions on the surface of the pelvis [35, 36].

The present study aims to address the shortcomings of previous approaches in quantifying pelvic symmetry, by observing deviations between 3D models of the left and right hemi-pelvises. The output is in the form of 3D deviation color maps (DCMs), which are a visual and quantitative representation of deviations between the left and right sides of the pelvis. The present method eliminates the use of landmarks or reference plates and thus removes the inter-user error associated with those approaches. A similar technique to the one applied in this study was also implemented to evaluate bilateral symmetry of the coronoid process [60] and the talus bone [11] and to evaluate asymmetry associated with spinal deformities such as scoliosis [61]. The objective of this paper is to provide a 3D quantitative measure to analyze bilateral symmetry of the pelvis. This can ultimately allow us to introduce a method for reconstruction of pelvic fractures by building fully intact patient-specific 3D pelvis models. By doing so, this work will help in providing a better treatment for these patients by offering quicker treatment proposals and easing the design process of custom plates for surgery.

The methods, tools and software used to evaluate left-right symmetry are first presented. Then, results including deviation statistics and DCMs for all test subjects will be presented, evaluating pelvic symmetry. We will then discuss deductions on pelvic symmetry, and the suitability of using virtual mirroring for unilateral pelvic fracture reconstruction.

3.3 Methods

Computed Tomography (CT) scan images of 14 pelvises (11 males, 3 females, age range from 18 to 24 years with a mean age of 20.6 years) were used in this study. These scans were performed using the Siemens SOMATOM definition flash scanner. As the scans were previously obtained

for clinical purposes and retrospectively reviewed for this work, the scanner parameters were not standardized across participants. The typical resolution was 512×512 pixels per slice and the average slice thickness was 1.57 mm (range: 1 – 2 mm). Approval was obtained from the Health Research Ethics Board at the University of Alberta including a waiver of consent to use the images retrospectively and anonymously in this study. To create 3D digitized models from these CT scan images, the scans were imported into Materialise-Mimics (Materialise®, Leuven, Belgium), an image processing software (Fig. 3.1a). A bone mask was created to isolate the bony tissue while eliminating all the soft tissue and some of the surrounding noise from the model (Fig. 3.1b). The spine and femurs were removed to isolate the pelvic bones. This was done by using a segmenting tool in Mimics® and detaching the pelvis from the spine and femurs by removing the pixels lying between them (Fig. 3.2). Finally, two masks were created, one for each side of the pelvis and the two 3D models were exported as separate STL files (Fig. 3.3).

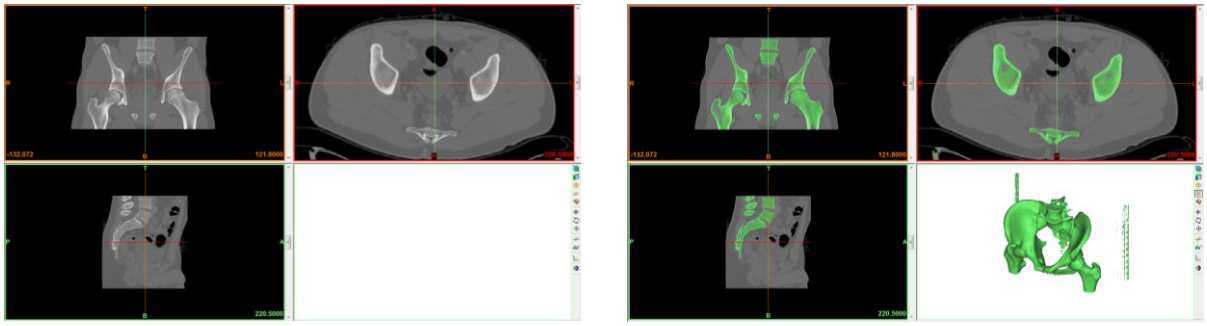

(a) **(b)**

Fig. 3.1 (a) Importing CT scan images into Mimics®. (b) Creating a bone mask.

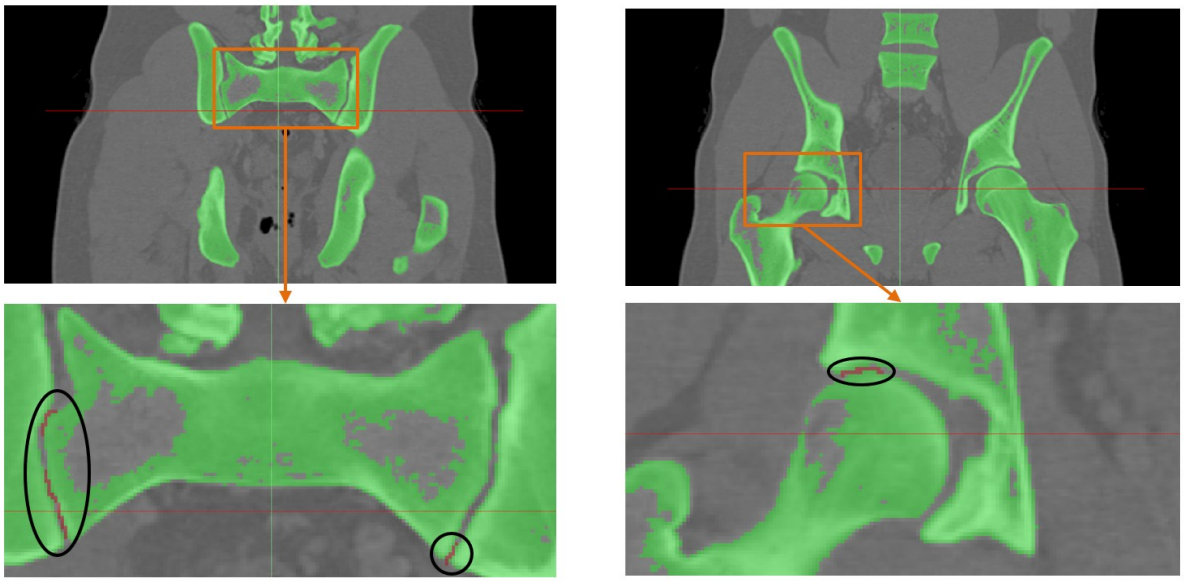

Fig. 3.2 Detaching the (a) spine and (b) femurs by removing the pixels (circled in black) between them and the pelvis in the coronal plane.

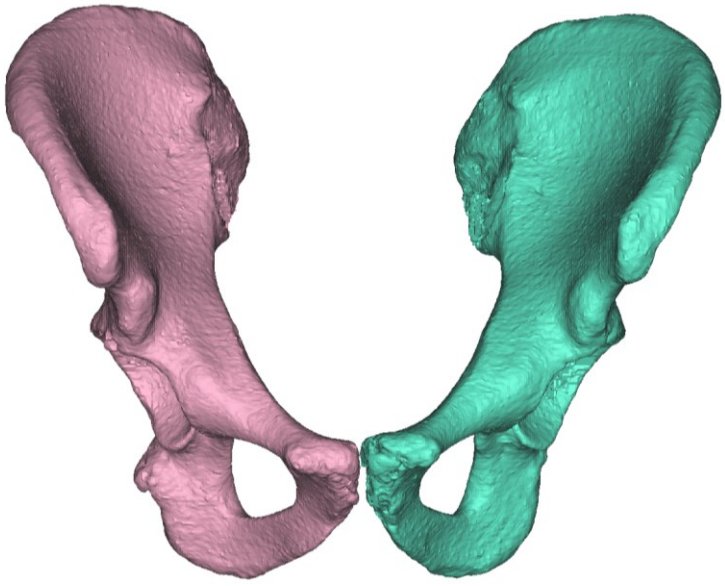

Fig. 3.3 Final 3D pelvis model created in Mimics®.

To compare symmetry of the left and right sides of the pelvis, the 3D models of either side were imported into Geomagic® Control™ 2014 (3D Systems, South Carolina, USA). By using a mirror function, the right side of the pelvis was reflected across the sagittal plane, defined by the YZ plane in the image coordinate system (Fig. 3.4). The reflected right side object was aligned with the left

side using the best-fit alignment function (Fig. 3.4). The best-fit alignment is a built-in function which minimizes the distance between two parts by means of an iterative closest point algorithm. In this analysis, the reference side of the pelvis was the left side (fixed), whereas the test side was the reflected right side (floating). After aligning both surfaces (reflected right side and left side), the geometrical deviations between them were determined by conducting a 3D deviation analysis on Geomagic®. This provides a DCM, a visual representation of the degree of difference between the surfaces (Fig. 3.5). The results showed both positive and negative deviations (orthogonal distances), indicating that the test surface (right pelvis half) was either above or below the reference surface (left pelvis half), respectively. A ± 2 mm deviation threshold was set for symmetry (green regions of the DCMs) and the upper and lower limits of the deviation color spectrum were set at ± 6 mm (red/blue regions of the DCMs). The output parameters of the 3D deviation analysis also included statistics, such as the root mean square (RMS) error, percentage of points in each sub range of the deviation spectrum, and the maximum upper and lower deviations.

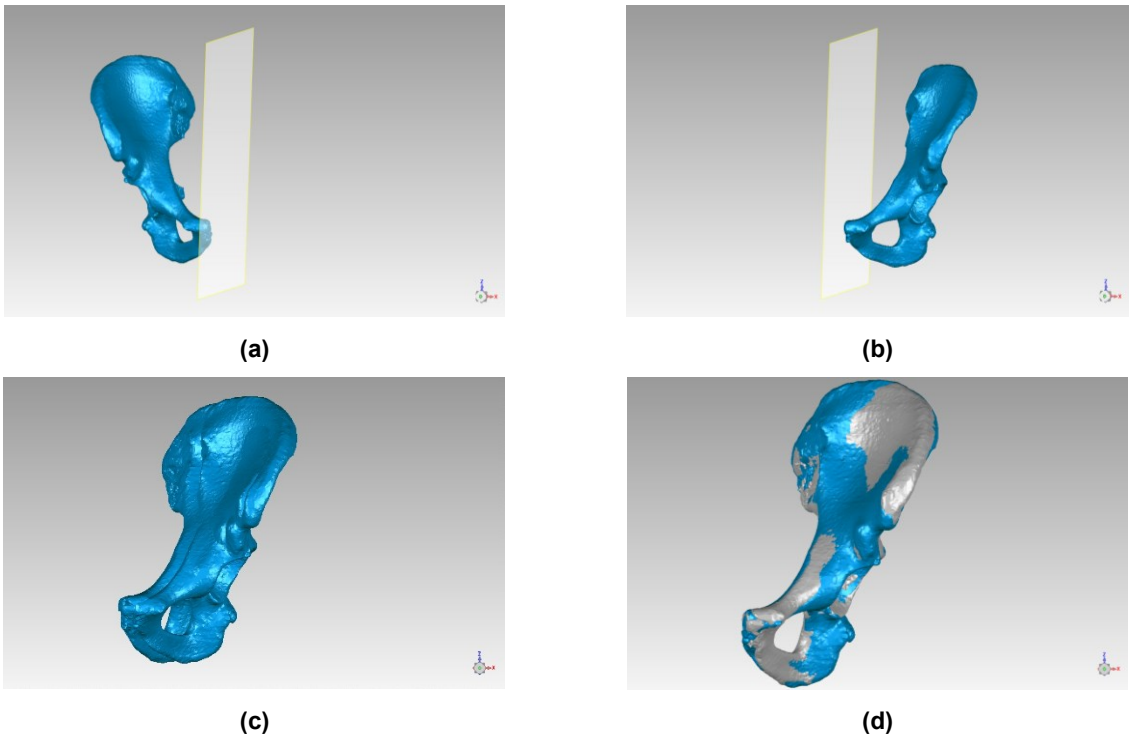

Fig. 3.4 Reflecting the right side of the pelvis across the sagittal plane in Geomagic®. (a) Before reflection. (b) After reflection. Aligning the reflected right side and left side of the pelvis in Geomagic®. (c) Before alignment, both models are shown in blue color. (d) After alignment, reflected right side is shown in blue color and left side is shown in grey color.

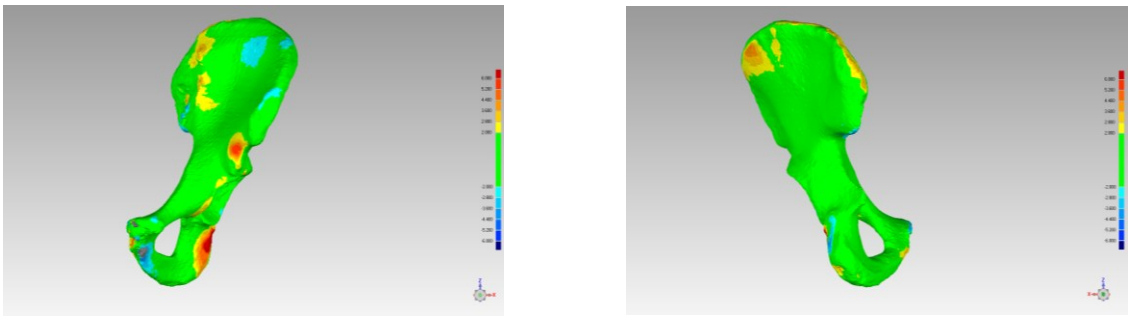

(a) (b)

Fig. 3.5 Color map produced by the 3D deviation analysis in Geomagic®. (a) Anterior view and (b) posterior view.

The volume and surface area of each hemi-pelvis was also obtained from Geomagic® Control™. It is important to note that the pelvis is constructed of cortical bone in the outer layer and cancellous bone on the inside. The volume calculated using Geomagic® is the volume of the material of a part, rather than the volume contained within the outline of the part. In order to allow for a fair comparison and to prevent differences in the depth of the cortical bone layer from impacting the results, the pelvis volume was filled to create a solid bone model.

Bilateral pelvic symmetry was evaluated based on (1) the mean RMS of the deviation, (2) the mean percentage of points below the $\pm$ 2 mm deviation threshold, and (3) differences in the surface area and volume between left and right hemi-pelvis models. Paired two-tailed t-tests with a significance level of $\alpha < 0.05$ were conducted using Microsoft Excel to evaluate differences in the surface area and volume between corresponding pelvis sides.

3.4 Results

Table 3.1 displays the volumes and surface areas of either side of the pelvises. The corresponding variations between the left and right sides were calculated and results show that the volumetric differences were less than 5.4% with an absolute difference of 1.94 $\pm$ 1.37 % (average $\pm$ SD). The differences in surface area were less than 2.6% with an absolute difference of 0.93 $\pm$ 0.75% (average $\pm$ SD). There were no statistically significant differences in volume ($p = 0.63$) or surface area ($p = 0.77$) between the left and right sides of the pelvic models.

The results of the deviation analysis between the reflected right side and left side are displayed in Table 3.2. It includes the root mean square (RMS), and the percentage of points within the $\pm$ 2 mm

range. The average RMS and percentage of points within ± 2 mm between the right and left side pelvic surfaces was 1.14 ± 0.26 mm and 91.9 ± 5.55%, respectively.

The DCMs for each subject are displayed in Fig. 3.6 and Fig. 3.7, showing both the anterior and posterior views of the pelvises. The green areas of the DCMs represent regions where the deviation between the left and right side surfaces are small (< 2 mm), whereas the red/blue areas of the DCMs represent regions with larger deviations (> 2 mm). It is important to note that positive deviation values indicate that the right side of the pelvis is above the left side (outward deviation) and negative deviation values indicate that the right side of the pelvis is beneath the left side (inward deviation).

Table 3.1 Volumes and surface areas of the right and left sides of the pelvises and the percentage differences between them. *Note: the average and standard deviation of the percentage difference are based on absolute values.

Subject	Sex (M/F)	Volume		Difference (%)	Surface Area		Difference (%)
		Right ($\times 10^5$ mm^3)	Left ($\times 10^5$ mm^3)		Right ($\times 10^4$ mm^2)	Left ($\times 10^4$ mm^2)	
S1	M	23.22	22.89	1.44	48.50	48.37	0.28
S2	M	47.36	45.84	3.21	70.83	69.30	2.16
S3	M	19.82	19.46	1.85	40.08	39.84	0.58
S4	M	36.19	36.09	0.27	62.25	61.93	0.52
S5	M	35.53	34.82	1.99	61.50	61.06	0.72
S6	M	38.45	38.30	0.41	63.70	63.92	-0.34
S7	F	26.37	26.71	-1.31	47.64	47.71	-0.13
S8	M	41.77	44.03	-5.39	68.29	70.03	-2.54
S9	F	28.27	28.97	-2.48	51.67	52.03	-0.70
S10	M	25.82	26.70	-3.40	47.56	48.45	-1.88
S11	M	46.59	45.96	1.37	73.31	72.86	0.61
S12	M	45.14	46.00	-1.91	70.44	71.31	-1.24
S13	M	31.83	32.38	-1.75	53.17	53.42	-0.46
S14	F	25.58	25.47	0.42	48.24	47.85	0.81
Average		33.71	33.83	1.94*	57.66	57.72	0.93*
SD		9.19	9.17	1.37*	10.77	10.77	0.75*

Table 3.2 Results of the deviation analysis (RMS is the root mean square deviation).

Subject	RMS (mm)	Percentage of points between ± 2 mm (%)
S1	1.20	91.4
S2	1.65	85.5
S3	1.13	92.5
S4	0.97	95.9
S5	1.13	92.5
S6	0.99	95.7
S7	0.76	98.8
S8	1.05	94.3
S9	0.91	97.3
S10	1.06	94.2
S11	1.43	85.0
S12	1.57	79.8
S13	1.24	87.0
S14	0.92	96.4
Average	1.14	91.9
SD	0.26	5.55

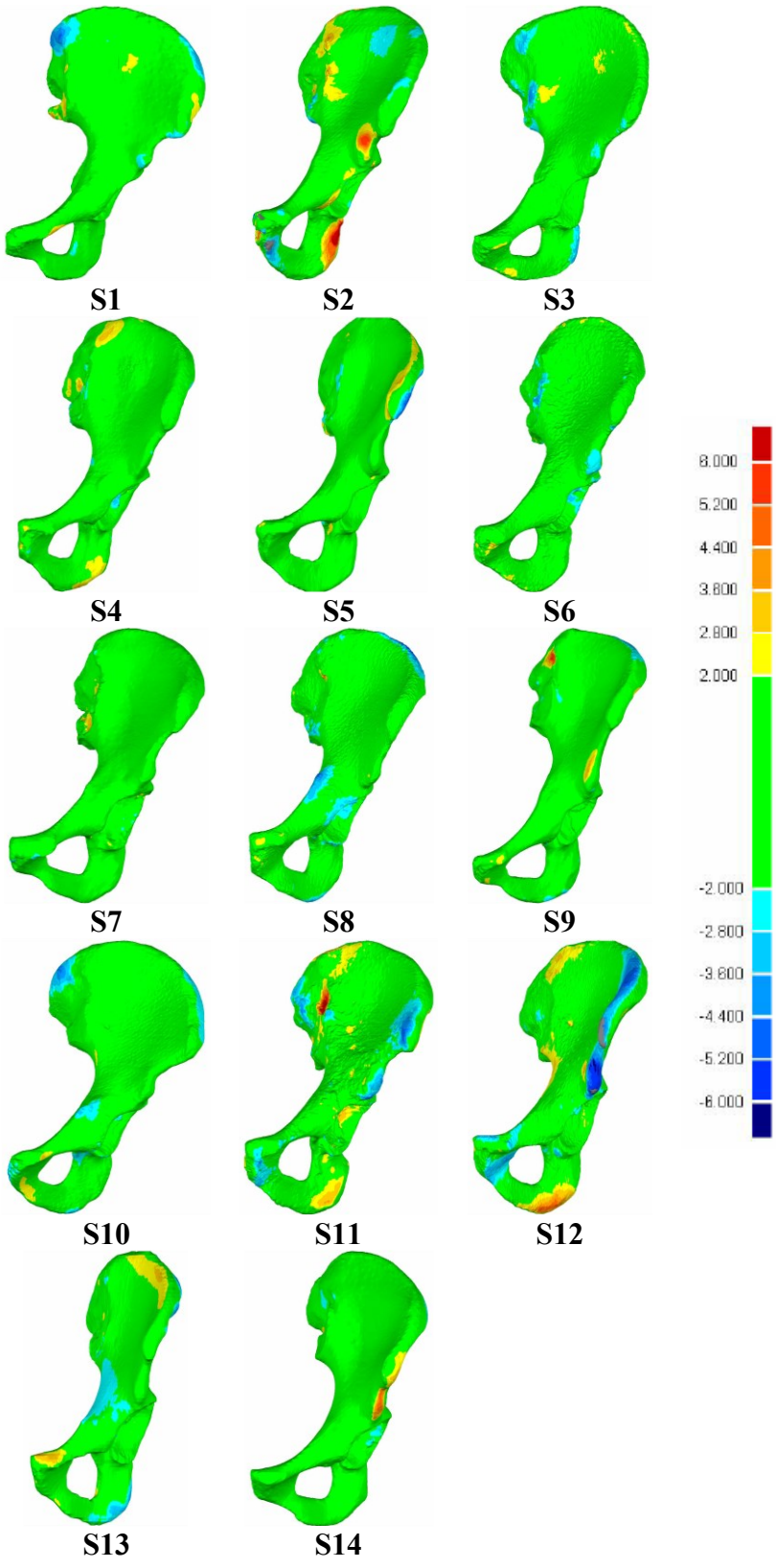

Fig. 3.6 Anterior view deviation color maps (mm) of the left side and reflected right sides of the pelvises.

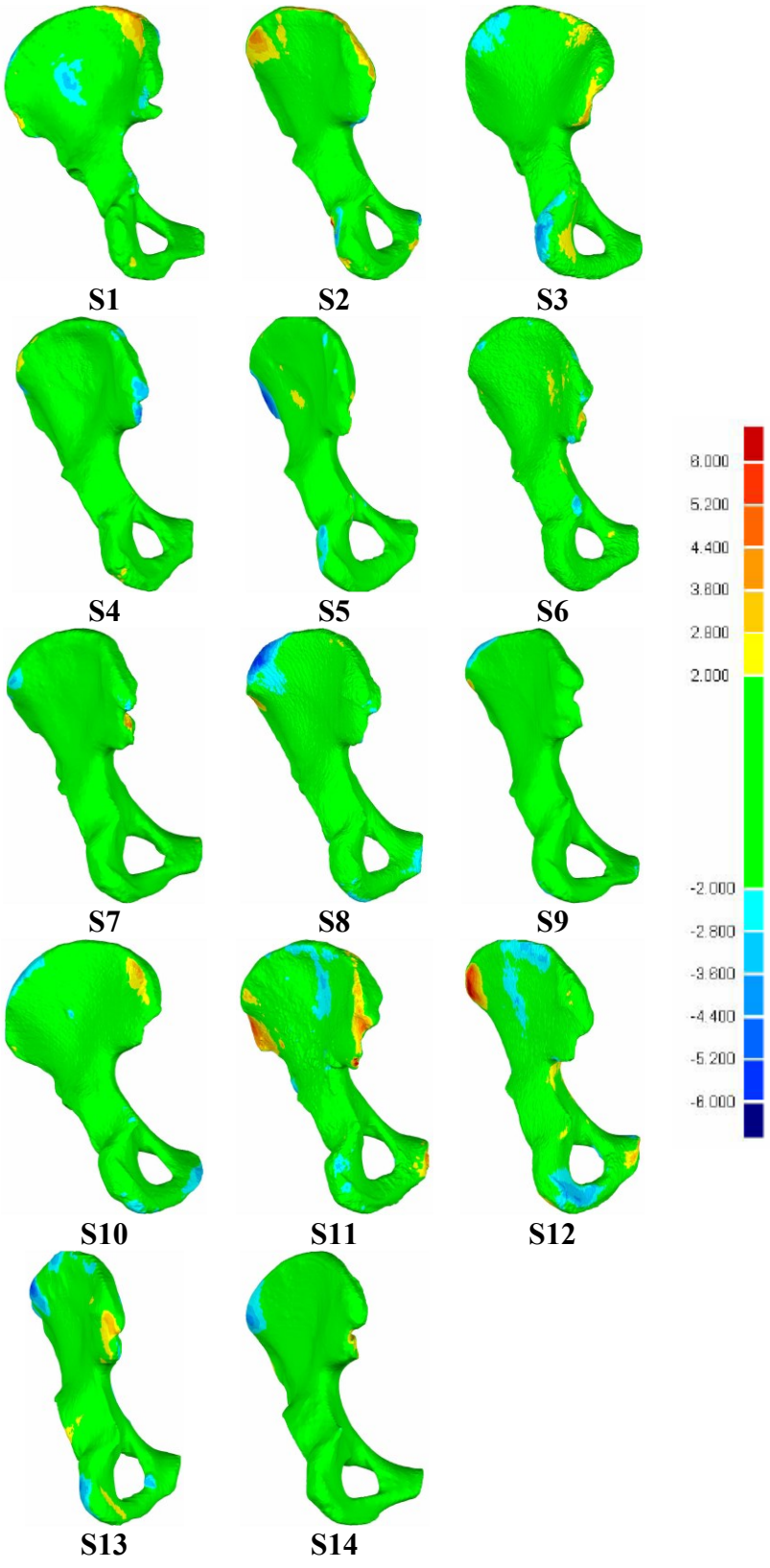

Fig. 3.7 Posterior view deviation color maps (mm) of the left side and reflected right sides of the pelvises.

3.5 Discussion

Studying pelvic symmetry and understanding the overall shape of the pelvis would aid surgeons in developing better treatment proposals. This would help in reducing the overwhelming mortality and morbidity statistics associated with pelvic fracture by enabling better surgical planning, reducing surgical operation time and surgical wait times, and providing more effective custom fixation plates [6]. Previous studies that focused on studying pelvic symmetry exploited the landmark method or pre-shaped implants [35, 36]. Boulay et al. used 71 variables (based on pelvic anatomical landmarks) to quantify left-right symmetry of 12 pelvic specimens and concluded that 56 of the variables are symmetric [35]. Osterhoff et al. confirmed that the periacetabular surface of the pelvis is symmetric by comparing the differences between either side of the pelvis and a virtual reference implant [36]. Despite their significance in the literature, these studies failed to capture the irregular geometrical shape of the pelvis [35, 36] and involved high intra- and inter-observer variability. To avoid these limitations, this work evaluated pelvic symmetry by examining the entire 3D geometric shape without using specific landmarks.

CT scan images of pelvises were converted to 3D models on Mimics® (Fig. 3.1 - Fig. 3.3) and exported to Geomagic® (Fig. 3.4 - Fig. 3.5) to conduct a symmetry analysis. The right pelvis side was reflected and aligned with the left side using a closest point algorithm and a 3D deviation analysis was performed to produce deviation color maps for each of the 14 subjects involved in the study. The volume and surface area of either side of the pelvises were also obtained from Geomagic® and percentage differences were calculated (Table 3.1). These volumetric and surface area differences between the left and right sides were small and showed no significant difference, suggesting that the pelvis is, indeed, symmetric. This aligns with the results obtained in previous studies [35, 36].

The deviation analysis produced many parameters to compare the left-right pelvic symmetry, including the maximum and average positive and negative deviations, the RMS values, as well as the percentage of points within each subrange of the deviation scheme (Table 3.2). These results also confirmed that the pelvis is symmetric, since the RMS values were small, on average (1.14 ± 0.26 mm). It is also important to note that the average percentage of points within the ± 2 mm range for all 14 test subjects was 91.9 ± 5.55% (average ± standard deviation), which further supports the conclusion of pelvic symmetry.

The DCMs (Fig. 3.6 and Fig. 3.7) produced by the deviation analysis provide a good visualization of the regions with high and low deviations. The specific areas of asymmetry were primarily localized to major muscle attachment sites including ischial tuberosities (hamstrings), iliac crests (gluteal muscles) and iliac spines. Minor variation in bone shape at these sites might be due to left-right differences in activation of these muscles. It is clear from these DCMs that the largest differences are in the ilia, particularly the iliac crests. Since these regions are non-articular, relatively high differences between the right and left surfaces would not affect the viability of the model. The acetabula, where the femur heads lie, are the only articular surfaces of the pelvis and are of the greatest concern in this context. The DCMs show that there are slightly high deviations (2.0 - 2.8 mm) in the acetabular regions of three of the test subjects (S6, S8 and S11). However, these deviations are not clinically significant to cause increased pressures in the joint contact areas between the femurs and acetabula as proven by Moody et al. on the talus bone contact areas [62].

There are several limitations to note in the present study. The digitization process involves manual segmentation in Mimics® and some of the CT scan images have considerable noise. Additionally, the CT scans of some of the subjects have larger slice thicknesses (2 mm) with a relatively small number of slices, which may affect the resolution of the images and 3D model. Therefore, the large deviations found in some areas of the DCMs may be a result of this or simply due to image artifacts. Since the images were obtained for clinical use, the scan parameters were not controlled across subjects. The study sample included 11 males and only 3 females. While, the male and female DCMs showed that there were also no observable differences between their pelvic symmetry, more test subjects would be needed in order to make a clear assessment. Future work will focus on increasing the sample size for both males and females, evaluating symmetry in specific pelvic regions such as the acetabulum and ilia, and developing a procedure to use symmetry to inform the reconstruction of pelvic fractures.

3.6 Conclusion

This study fills a crucial gap in the literature as it quantifies pelvic symmetry, allowing surgeons to confirm the effectiveness of using the mirroring tool in the virtual surgical planning process. The results obtained show that the right and left sides of the pelvis have a high degree of symmetry. The average volume and surface area differences between either side of the pelvises were small,

1.94 ± 1.37 % and 0.93 ± 0.75%, respectively. The highest deviations between right and left pelvic surfaces were found on non-articular surfaces, primarily iliac and ischial muscle attachments. Only three subjects had slightly high deviations on the articular surfaces of the pelvis, the acetabular regions. However, these deviations are clinically insignificant in the context of using the contralateral pelvic model for surgical planning. As a result, it would be reasonable to apply the concept of pelvic symmetry to create fully intact patient-specific 3D models of pelvises using an unfractured contralateral side. The technique described in this paper for evaluating left-right symmetry of the pelvis can be extended to other parts of the human body, which further demonstrates the potential importance of this work.

Chapter 4: Reconstruction for Unilaterally Fractured Pelvises

This chapter was published in the International Journal of Computer Assisted Radiology and Surgery:

Ead MS, Westover L, Polege S, McClelland S, Jaremko JL, Duke KK (2020) Virtual reconstruction of unilateral pelvic fractures by using pelvic symmetry. Int J Comput Assist Radiol Surg 15:1267–1277. https://doi.org/10.1007/s11548-020-02140-z

4.1 Abstract

Purpose: Pelvic fractures are known to be one of the most difficult injuries to treat. The objective of this study is to introduce a novel technique for virtual unilateral pelvic fracture reconstruction. Since the pelvis exhibits remarkable left-right symmetry, the contralateral hemipelvis can be used as a template for rebuilding the fractured hemipelvis.

Methods: CT scan data of the pelvic region of eight subjects with acute unilateral pelvic fractures were involved in this study. Computer-aided design (CAD) software was used to create 3D models of these pelvises. The contralateral hemipelvis of each subject was then reflected across the sagittal plane and the fractured hemipelvis was rebuilt by aligning the bone fragments with their equivalent location on the reflected side. To evaluate the quality of this reduction process, a 3D deviation analysis was conducted to calculate the differences between the reflected intact hemipelvis and the reconstructed hemipelvis.

Results: Results showed that the average root mean square (RMS) of deviations and average percentage of points within a ± 2 mm predefined threshold was 1.32 ± 0.22 mm and 88.4 ± 3.78%, respectively. The deviation color maps (DCMs) obtained indicated that the largest differences were along the fracture lines and on the non-articular surfaces of the pelvises.

Conclusion: These results allowed us to conclude the validity of this procedure, since the average RMS difference was below 2 mm and the average percentage of points within ± 2 mm was high. The proposed technique will allow surgeons to provide their patients with more accurate reconstruction procedures which can potentially improve surgical outcomes.

4.2 Introduction

Computer-aided surgery (CAS) is increasingly used to assist in surgical planning with the goal of improving outcomes [37]. A benefit of CAS is data-sharing with distant practitioners, allowing for more informed decisions to be made [38]. One application of CAS is in craniofacial surgeries, where computer-aided design (CAD) software is used to create three-dimensional (3D) geometric computer models. These models can then be used to develop treatment protocols and simulate them in a virtual environment [38]. CAS has also shown to provide more accurate leg alignment in total knee arthroplasty, which is a crucial step for the long-term success of this surgery [39]. Another application of CAS is in oral implantation, where 3D models are utilized in the planning process and outperform manual planning techniques which only use two-dimensional (2D) images [40].

Pelvic fractures, particularly those in the acetabular region, are challenging for orthopedic surgeons [11]. This is due to complex pelvic anatomy and limited surgical access to its articular surfaces [10, 11, 18, 63, 64]. CAS has been introduced into pelvic fracture reconstruction surgeries to overcome these limitations and enhance results [11, 18, 41, 63, 64]. Typically, computerized tomography (CT) scans are first converted into 3D models using different computer software and segmentation tools are used to isolate the bone fragments. The pelvises are then reduced by virtually moving the individual pieces into the appropriate position and orientation. Fixation plates can then be contoured over the reduced pelvis and screws fitted accordingly [10, 18, 41–45]. This preoperative planning technique addresses the limitation of prolonged operation times associated with bending the fixation plates during the surgery [34]. Another study also proposed a method for shaping pelvis fixation plates by 3D printing the uninjured hemipelvis and contouring the plates over the printed model. Although this study also addresses the limitation of prolonged operation times, there was no technique for precisely identifying the location of the fractures on the uninjured hemipelvis, which could potentially affect the quality of the reduction [46]. Despite the advantages that the former method offers over conventional surgical techniques, it also has its weaknesses. Currently, virtual pelvis reduction is subjective, time consuming and requires expert medical knowledge to perform, which is not always feasible [10, 42, 44, 45, 65]. In addition, the virtual reconstruction is not performed with reference to the patients' intact hemipelvis, which can

potentially affect the quality of the reduction. To overcome these drawbacks, we propose a new technique for pelvic fracture reconstruction that utilizes pelvic symmetry.

Human bilateral symmetry refers to parts of the body being mirror images of their opposite sides. This concept is useful in varied ways including estimating skeletal age and studying the effect of facial symmetry on attractiveness [29, 53]. Bilateral symmetry of bones has also been helpful in orthopedics, where the intact bone serves as a template for the contralateral bone in the reconstruction process [27, 59]. Previous studies have quantified left-right symmetry of the pelvis and have concluded that it is symmetric [35, 36, 66]. Knowing this, the same concept may be applied to reconstruct unilaterally fractured pelvises by reflecting the uninjured hemipelvis across the sagittal plane to provide a model for the fractured hemipelvis.

Utilizing bilateral symmetry in pelvis reconstruction would eliminate the shortcomings of the current reconstruction techniques noted previously. It would preserve the pelvis' natural geometry, which will allow surgeons to develop more fully customized fixation plates for surgery. It can be a semi-automatic reconstruction method, limiting time and observer subjectivity. Also, it only requires basic computer software skills and is not contingent on the presence of a surgeon or medical expert in the field.

Therefore, the objective of this work is to outline a method for virtually reconstructing unilaterally fractured pelvises by using the contralateral side as a template. The product will be a complete 3D model of a pelvis which can then be used to develop customized fixation plates and plan the surgical procedure.

4.3 Methods

A set of 8 adult patients (5 males, 3 females, age range from 20 to 43 years with a mean age of 29.9 years) with acute unilateral displaced pelvic fractures was identified from a tertiary hospital archive. Approval from the Health Research Ethics Board was obtained with a waiver of consent to use the data anonymously. The data was in the form of pelvic region CT scan images. The scans were performed for clinical use on either the Siemens SOMATOM Definition AS+ scanner or the General Electric Medical Systems LightSpeed VCT scanner. The average pixel size of the CT scan images was 0.744 mm (range: 0.572 – 0.977 mm) with a resolution of 512×512 pixels per slice.

The average number of slices for the CT scan data sets was 206 (range: 103 – 322) and the average slice thickness was 1.469 mm (range: 1 – 2.5 mm).

A representative example of a patient with an iliac fracture on the left hemipelvis will be used to demonstrate the digitization and reconstruction procedure. The CT scan images of each patient were digitized into 3D models with the use of Mimics® image processing software (Materialise®, Leuven, Belgium) following a similar procedure to our previously reported work [66]. The images were imported into Mimics® (Fig. 4.1a) and a predefined bone mask (colored in green) was applied to isolate the bony tissue from the soft tissue (Fig. 4.1b). The noise surrounding the pelvic region was removed by using a region growing tool. One point on the pelvis was selected and all regions connected to it were included in the new mask (colored in yellow), whereas the points floating around were excluded (Fig. 4.1c). Since the pelvic region includes other bones, such as the spine and femora (Fig. 4.1d), these are separated from the pelvis with a manual segmentation tool in Mimics®. The individual pixels attaching these bones together are eliminated (Fig. 4.2) and the same segmentation tool is also used to detach the fractured pieces from one another (Fig. 4.3). Masks are then created for the intact side of the pelvis and each of the fractured pieces (Fig. 4.4) and saved as separate STL files. The final 3D pelvis models created in Mimics® for all test subjects are shown in Fig. 4.5 in both anterior and posterior views.

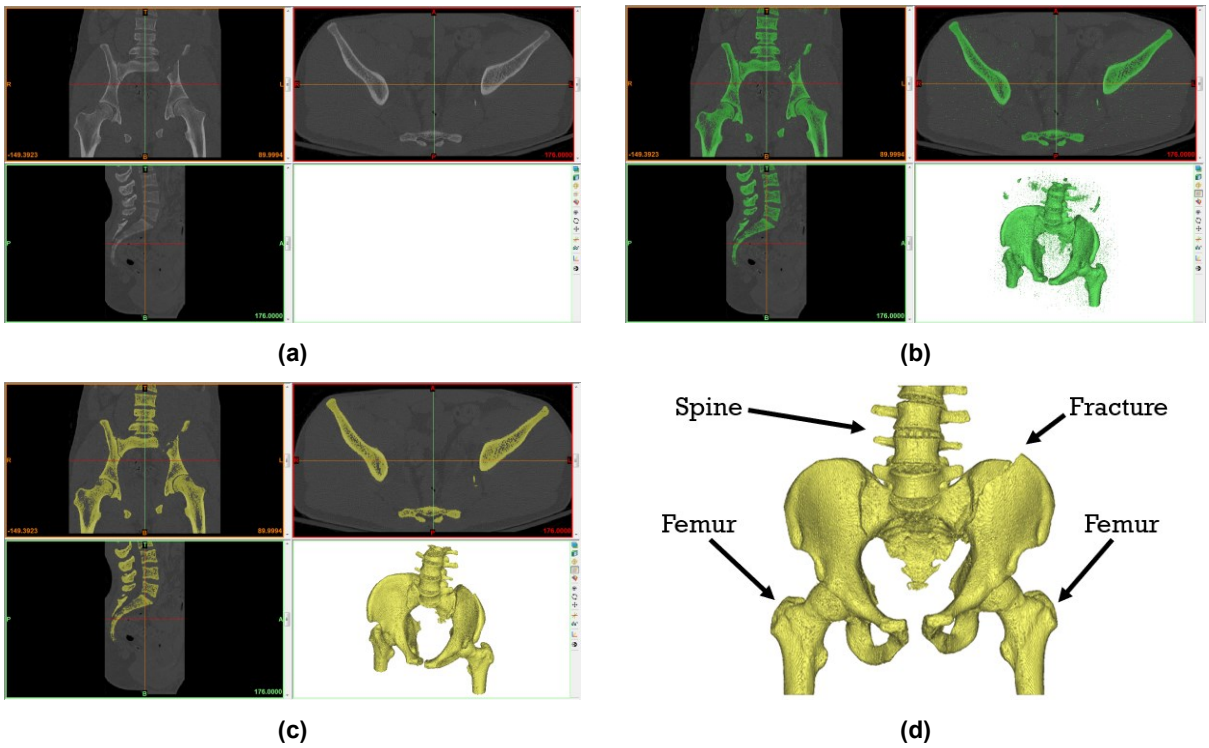

Fig. 4.1 (a) Importing CT scan images into Mimics®. (b) Creating a bone mask. (c) Removing surrounding noise. (d) Anterior view of pelvic bone model with spine and femurs.

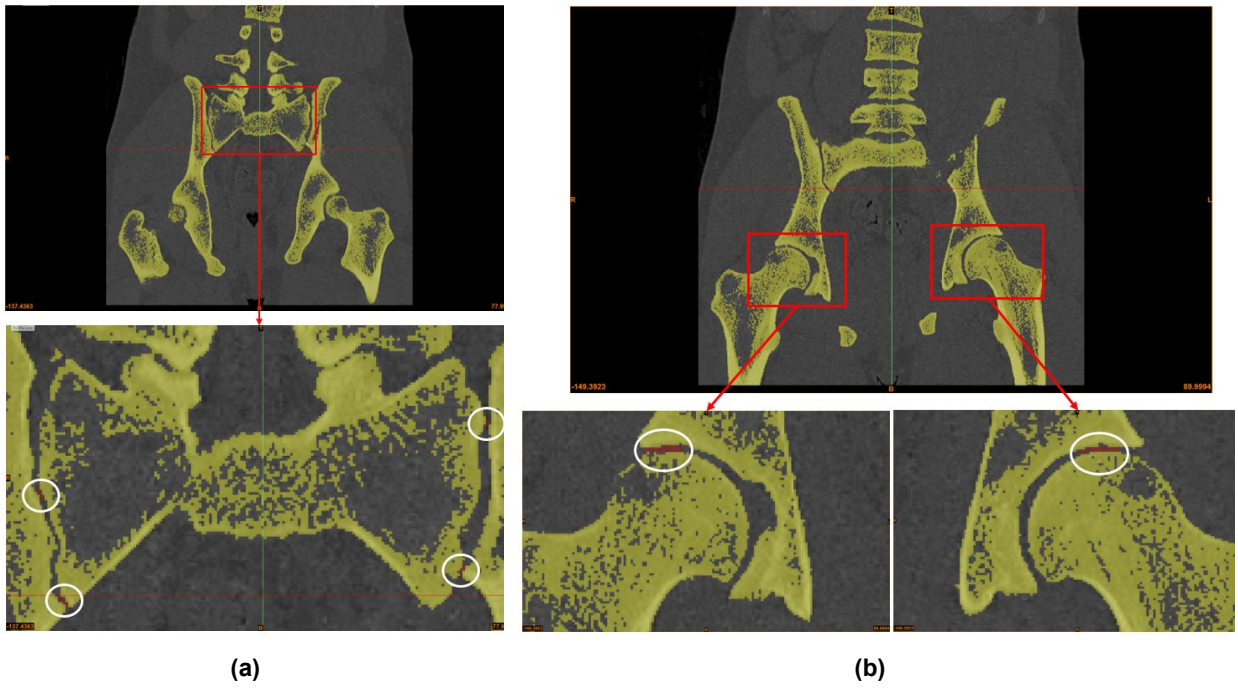

Fig. 4.2 Detaching the (a) spine and (b) femurs by removing the pixels (circled in white) between them and the pelvis in the coronal plane.

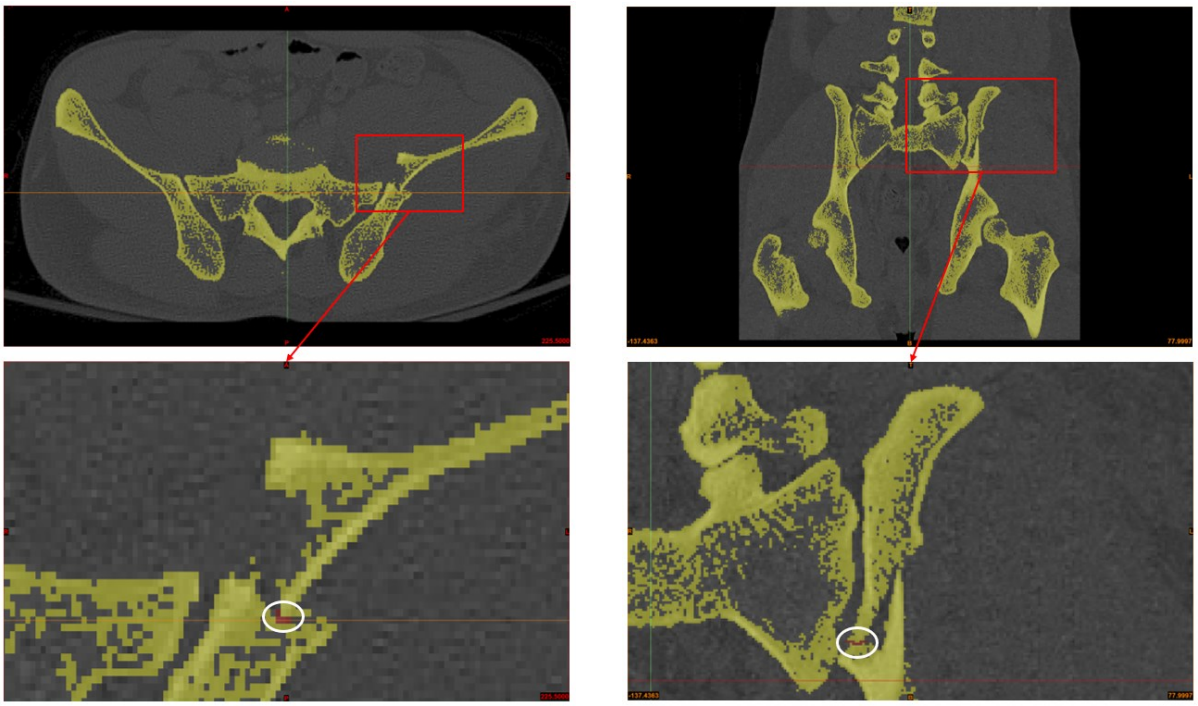

(a) (b)

Fig. 4.3 Separating the fractured pieces by removing the pixels (circled in white) between them in the (a) axial plane and (b) coronal plane.

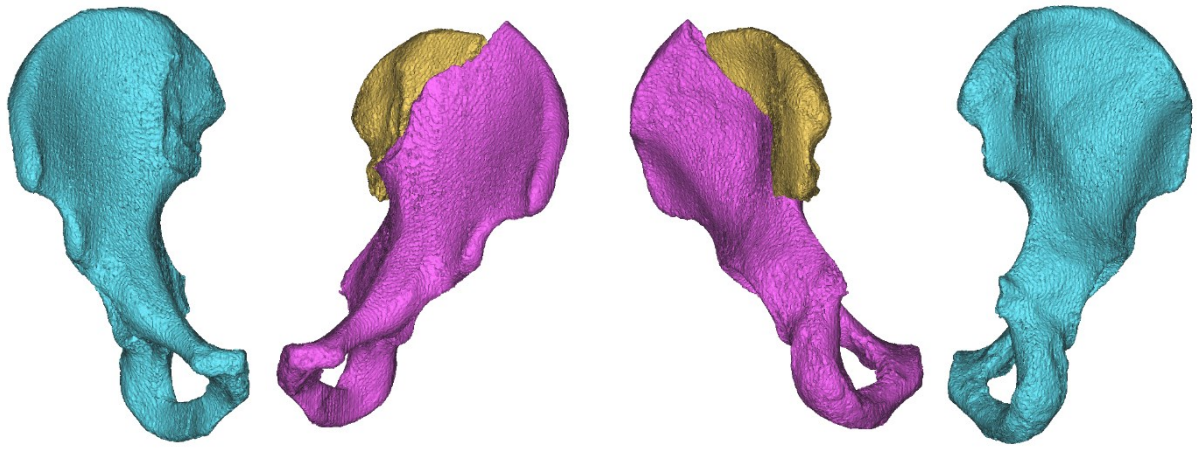

(a) (b)

Fig. 4.4 Final 3D pelvis model created in Mimics® (a) anterior view and (b) posterior view.

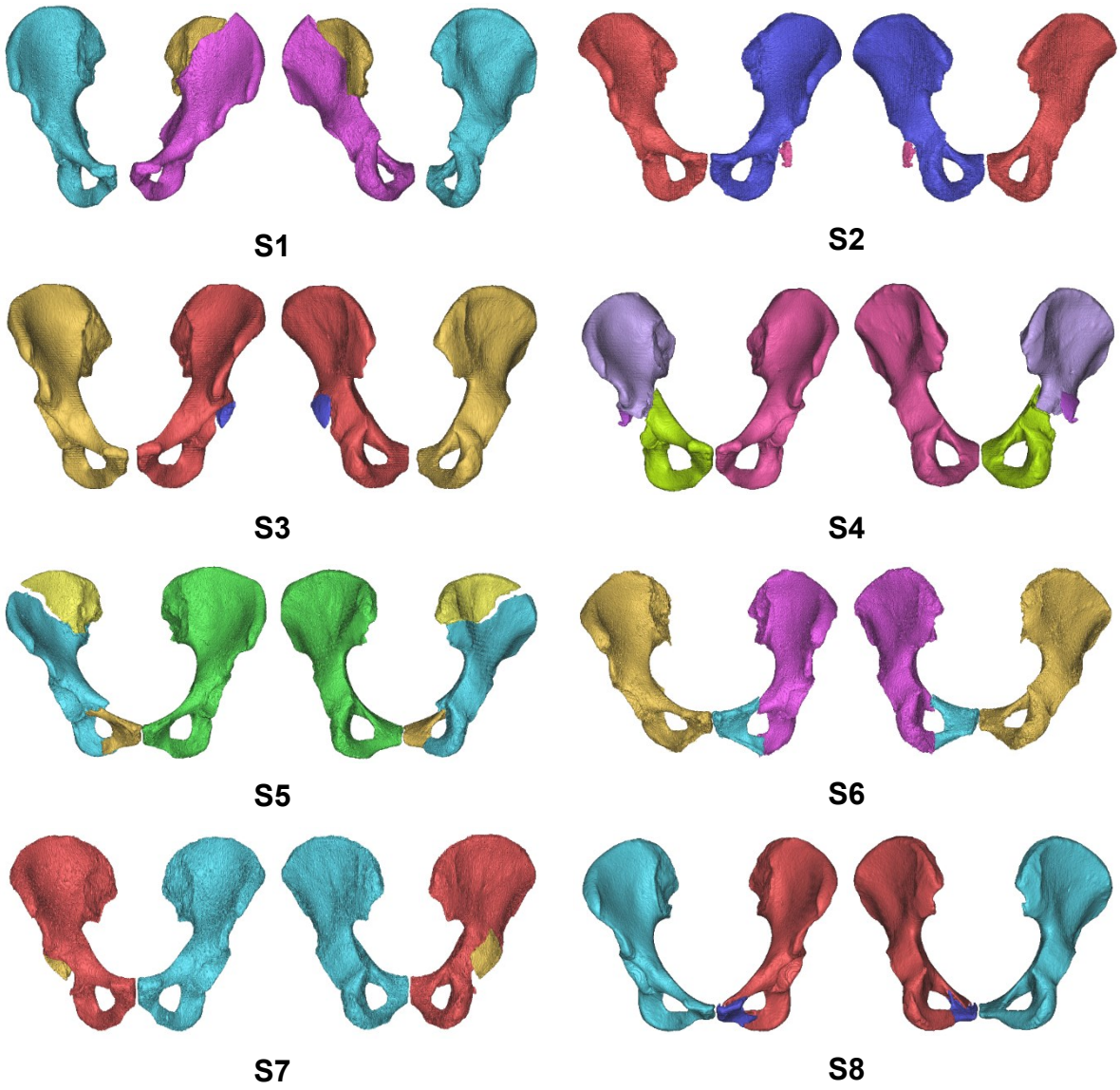

Fig. 4.5 Final 3D pelvis models for all subjects created in Mimics® (anterior view on the left and posterior view on the right). The location of the bone fragments in these images are the way they appear exactly in the CT scan images, i.e. they were not virtually moved out of place.

In order to reconstruct the fractured side of the pelvis, a CAD software known as Geomagic® Control™ 2014 (3D Systems, South Carolina, USA) is utilized. The intact side and fractured pieces are all imported into this software. A mirror function in Geomagic® is used to reflect the intact side of the pelvis across the sagittal plane (Fig. 4.6). The fractured side is reconstructed by selecting the equivalent region on the intact side to serve as a template (Fig. 4.7). The pieces were aligned with the template by employing a best-fit alignment function in Geomagic® (Fig. 4.7); this minimizes the distance between two surfaces by use of an iterative closest point algorithm. Once

all fractured pieces are aligned, the reconstructed side and reflected intact side are saved as two separate STL files. Next, the entire reconstructed side is aligned with the intact side by using the same best-fit alignment function (Fig. 4.8). A 3D deviation analysis is then conducted using Geomagic® to calculate the geometrical deviations between the two surfaces (reconstructed and reflected intact sides) [66]. The 3D deviation analysis produces a deviation color map or DCM (Fig. 4.9), the root mean square (RMS) of deviations, and the percentage of points within each subrange of the deviation spectrum. These parameters were used to assess the validity of this technique.

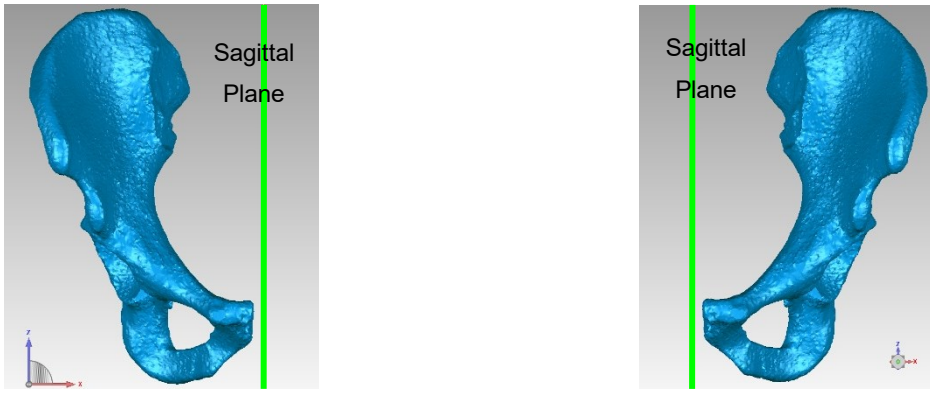

(a) **(b)**

Fig. 4.6 Reflecting the intact side of the pelvis across the sagittal plane (green line) in Geomagic®. (a) Before reflection and (b) after reflection.

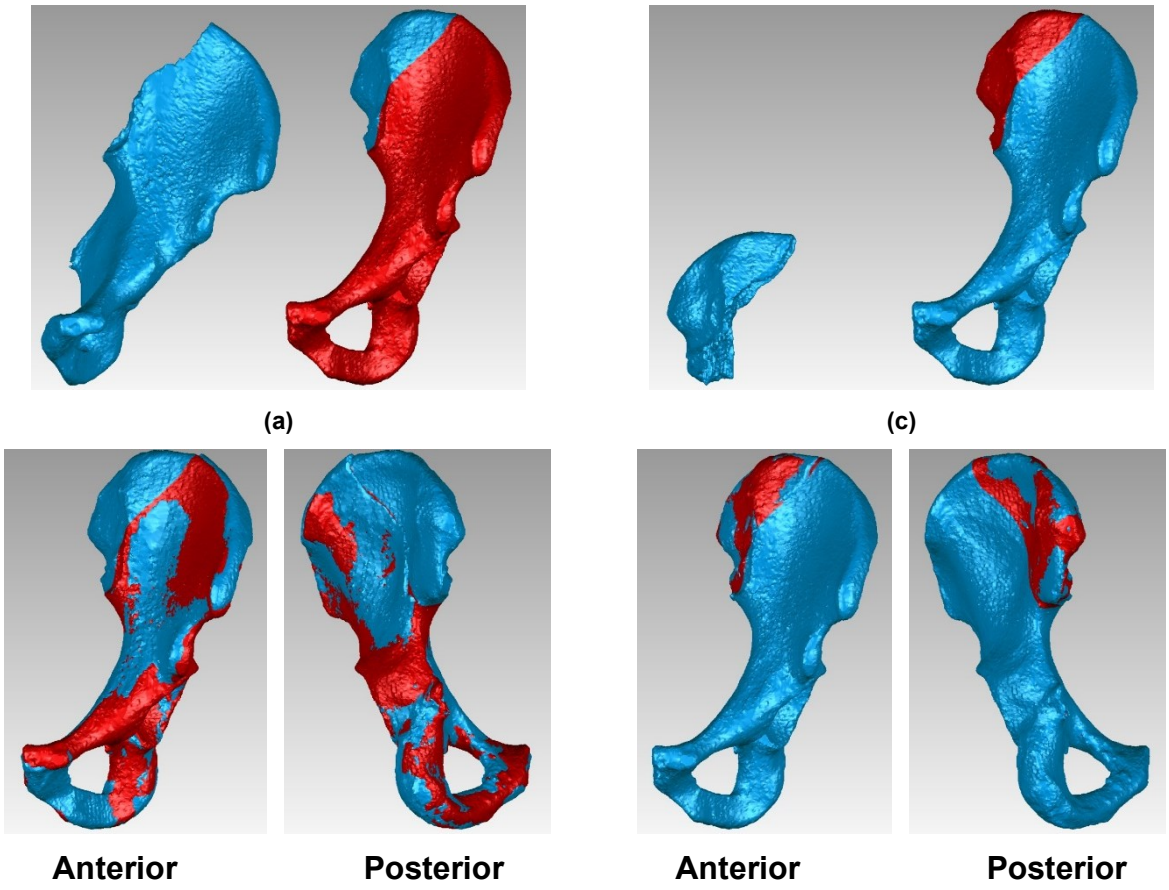

Fig. 4.7 Aligning the fractured pieces and intact side of the pelvis in Geomagic®. (a) Fractured piece 1 and intact side with reference region highlighted in red. (b) Fractured piece 1 aligned with reference region on intact side. (c) Fractured piece 2 and intact side with reference region highlighted in red. (d) Fractured piece 2 aligned with reference region on intact side.

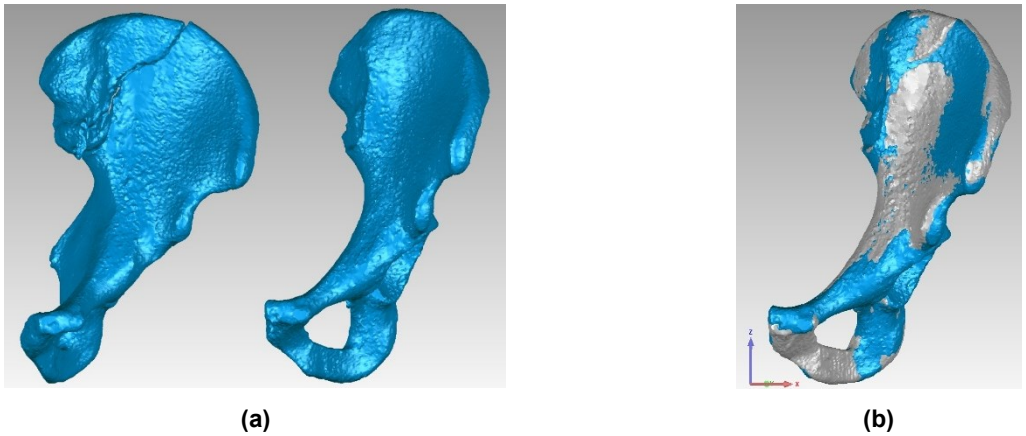

Fig. 4.8 Aligning the reconstructed side and intact side of the pelvis in Geomagic®. (a) Before alignment. Both models are shown in blue. (b) After alignment. Reconstructed side is shown in grey and intact side is shown in blue.

DCMs are visual representations showing the degree of difference between two surfaces, with the use of colors. In this respect, deviations can be positive or negative; for positive deviations, the test surface (reconstructed side) is above the reference surface (intact side) and vice versa for negative deviations. In order to quantitatively analyze and compare the results, a threshold of ± 2 mm deviation was specified [66]. This threshold is based off results in the literature which concluded that a reduction within 2 mm is considered acceptable in terms of preventing osteoarthritis in the hip joints [11, 16]. Therefore, points below ± 2 mm (green regions of the DCMs) were considered adequate for this method and points between ± 2 mm and ± 6 mm (red/blue regions of the DCMs) were considered high. In addition to the DCMs, the outcome parameters for the reconstructions were the RMS of the deviations and the percentage of points below ± 2 mm deviation.

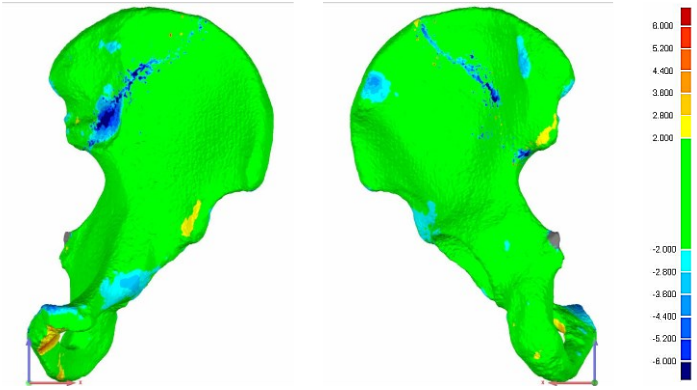

Fig. 4.9 Color map of Subject 1 produced by the 3D deviation analysis in Geomagic®, using the automatic symmetric registration technique. (a) Anterior view and (b) posterior view.

The automatic symmetric registration technique used in the reconstruction procedure outlined was not the only technique tested. Initially, we attempted a manual point-to-point alignment method on the same subject (Subject 1) on Geomagic®. In this method, the user selects points on the fractured surfaces of each of the pelvic pieces, bringing the two pieces together (Fig. 4.10). A minimum of 3 points (on each side) needs to be selected for the pelvis to be reconstructed. After pelvis reduction, a 3D deviation analysis was conducted to evaluate the differences between the reflected intact hemipelvis and the reconstructed hemipelvis. The DCM obtained is shown in Fig. 4.11; the RMS and percentage of points between the ± 2 mm threshold was also recorded, in order

to illustrate the differences between both techniques (automatic symmetric registration and manual point-to-point alignment).

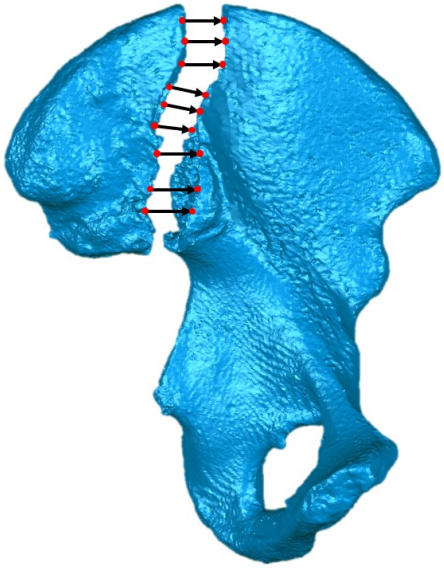

Fig. 4.10 Manual point-to-point reconstruction technique. Points on each of the fractured surfaces (red dots) are selected and the pieces are joined at those locations.

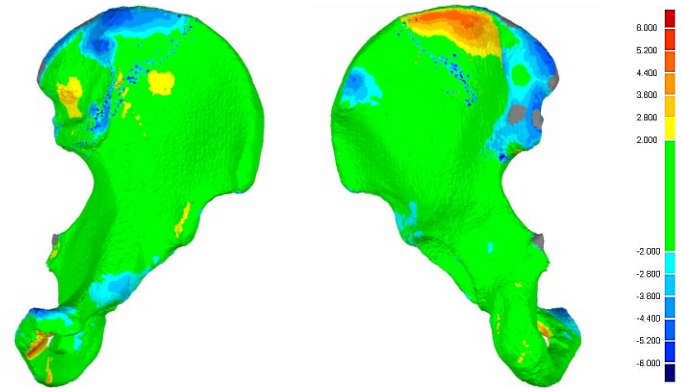

(a) **(b)**

Fig. 4.11 Color map of Subject 1 produced by the 3D deviation analysis in Geomagic®, using the manual point-to-point alignment technique. (a) Anterior view and (b) posterior view.

4.4 Results

The deviation analysis for Subject 1 using the manual point-to-point alignment method showed that the RMS of deviations and percentage of points between ± 2 mm was 1.62 mm and 80.6%, respectively. The results of the deviation analysis between the reconstructed and intact sides using the automatic symmetric registration technique for all subjects are displayed in Table 4.1. The RMS and the percentage of points within the ± 2 mm range are also reported. Results showed that the average RMS and average percentage of points within the ± 2 mm threshold between the reconstructed and intact pelvic surfaces was 1.32 ± 0.22 mm and 88.4 ± 3.78% (average ± standard deviation), respectively.

DCMs for all subjects are displayed in Fig. 4.12 (anterior view) and Fig. 4.13 (posterior view). Fig. 4.14 includes the side view DCMs of the subjects with acetabular fractures. As discussed, the green regions of the DCMs represent areas where the differences between the reconstructed and intact pelvis surfaces are small (< 2 mm), whereas the red/blue regions of the DCMs represent areas where differences are large (> 2 mm).

Table 4.1 Results of the deviation analysis (RMS is the root mean square deviation).

Subject	Sex (M/F)	RMS (mm)	Percentage of points between ± 2 mm (%)
S1	M	1.39	89.2
S2	M	1.26	91.2
S3	M	1.27	88.5
S4	M	1.48	81.9
S5	F	1.56	86.6
S6	F	1.33	86.0
S7	M	1.42	89.1
S8	F	0.84	94.7
Average		**1.32**	**88.4**
SD		**0.22**	**3.78**

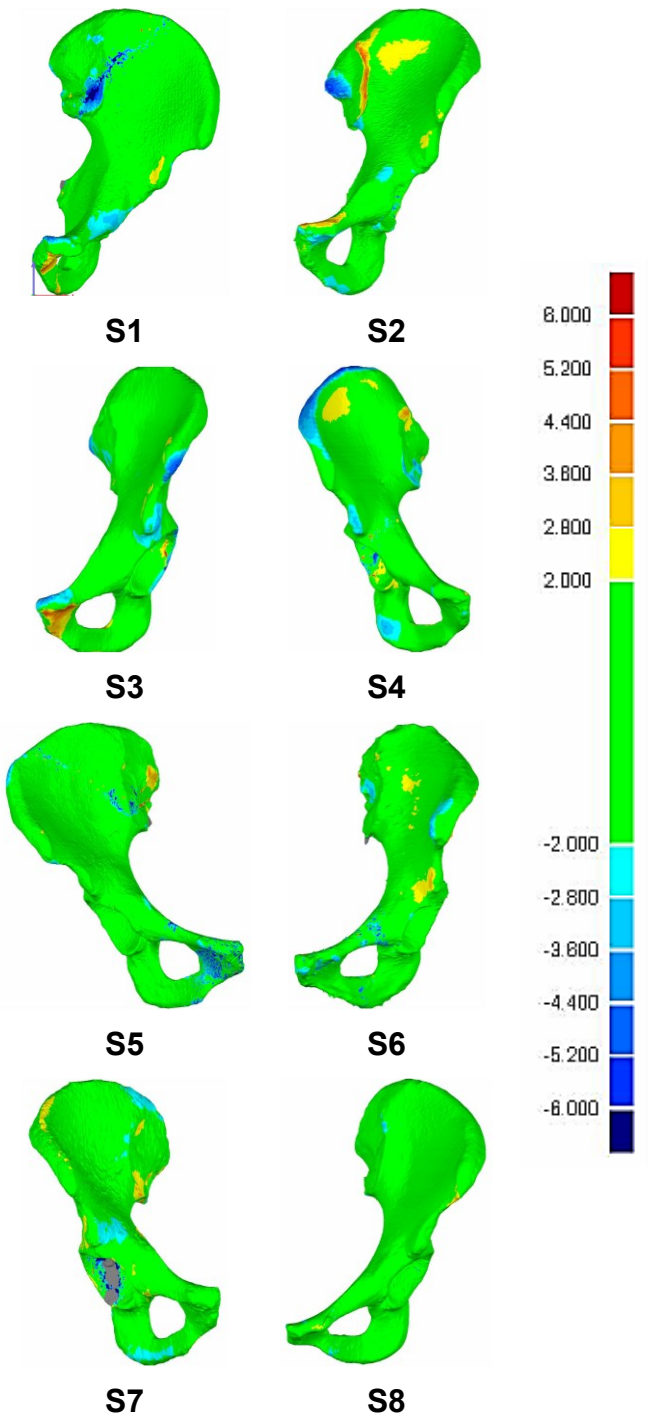

Fig. 4.12 Anterior view deviation color maps (mm) of the reconstructed and intact sides of the pelvises.

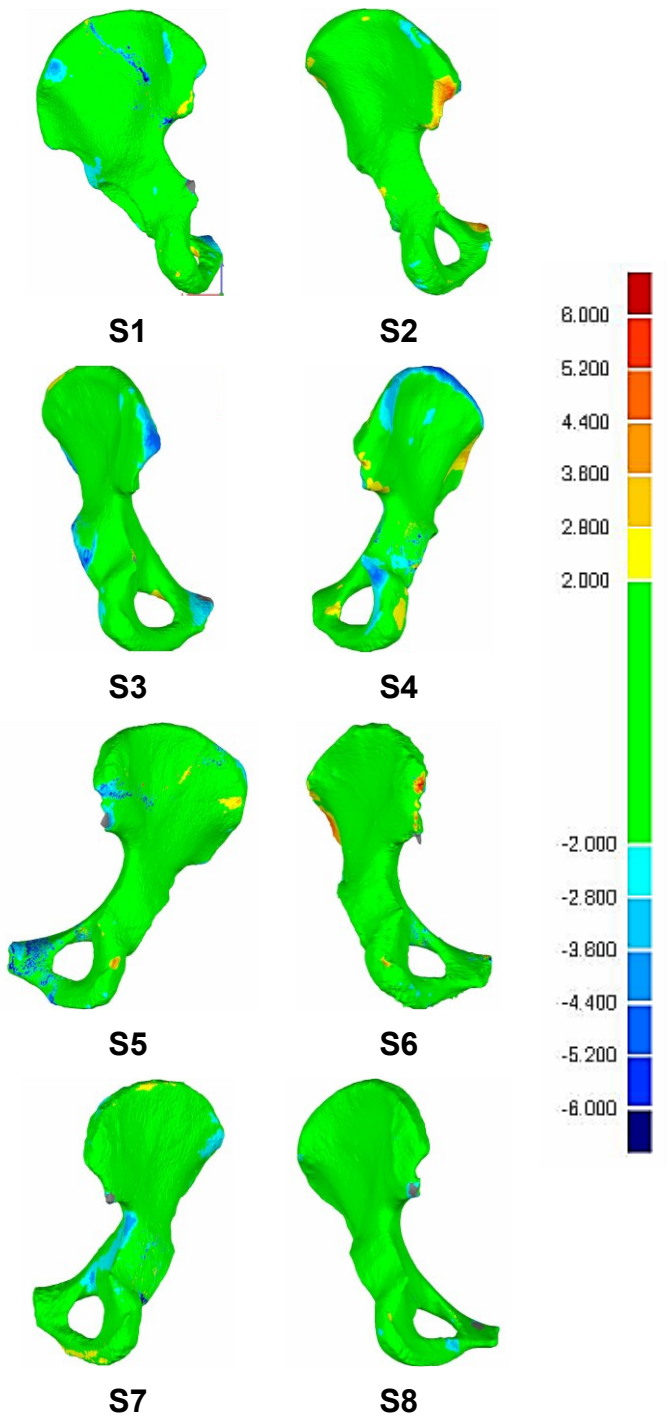

Fig. 4.13 Posterior view deviation color maps (mm) of the reconstructed and intact sides of the pelvises.

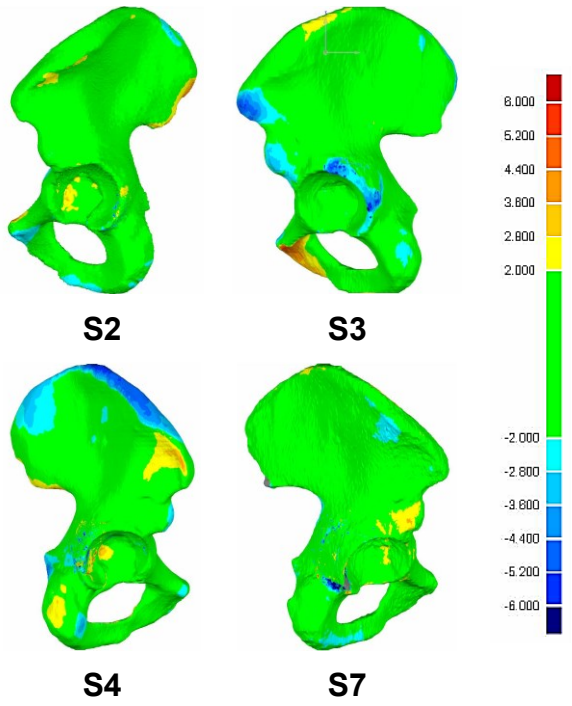

Fig. 4.14 Side view deviation color maps (mm) of the reconstructed and intact sides of the pelvises with acetabular fractures.

4.5 Discussion

Virtually reconstructing pelvises by creating 3D models can assist surgeons in the surgical planning process and allow them to provide more precise treatment proposals. This has the potential to reduce patient operation times, which typically increases the risk on the patient when prolonged. Although previous studies have highlighted the importance of virtual pelvis reconstruction and the numerous benefits it offers, the techniques outlined have certain deficiencies [10, 11, 18, 63, 64]. The methods defined in the literature do not preserve pelvis symmetry and involve high observer subjectivity. In addition, a medical professional is needed for the virtual reduction step. Consequently, the methods proposed in this work aim to address these issues.

Since the pelvis exhibits remarkable left-right symmetry [66], using the intact hemipelvis to serve as a template for reconstructing the fractured hemipelvis was the key inspiration behind this work. Mimics® was used to create 3D models of the unilaterally fractured pelvises from CT scan images (Fig. 4.5). These pelvises were then reconstructed on Geomagic® by reflecting the intact side and using it as a template for the fractured side (Fig. 4.6).

After reconstructing the fractured pelvises (Fig. 4.7 - Fig. 4.8), a deviation analysis was performed between the reconstructed and intact hemipelves for each test subject in Geomagic®. This provided several parameters from which we were able to assess the suitability of this reconstruction technique. The parameters included the RMS and percentage of points within the ± 2 mm preset threshold (Table 4.1), which averaged at 1.32 ± 0.22 mm and 88.4 ± 3.78%, respectively. These results allowed us to conclude that this reconstruction technique is acceptable, since the average RMS was well below 2 mm and the average percentage of points within ± 2 mm was high. The results also closely match those found in our previous work which compared left-right pelvic symmetry [66]. Intact pelvises were used in the previous work and the geometrical differences between the reflected right side and left side were recorded. The average RMS and average percentage of points within ± 2 mm was 1.14 ± 0.26 mm and 91.9 ± 5.55%, respectively [66]. This supports the validity of the proposed technique for fracture reconstruction.

The deviation analysis also produced DCMs, which allowed us to easily visualize the locations with the highest and lowest differences between the reconstructed and intact sides (Fig. 4.12 - Fig. 4.14). The highest deviations in all test subjects were along the fracture lines. Slightly high deviations (2.0 - 2.8 mm) were found in the ilia of some subjects, which could be due to the presence of major muscle attachments in those regions. These deviations could also be a result of plastic deformation from high energy trauma. However, the ilia are non-articular surfaces of the pelvis, thus, slightly high deviations in these regions are not necessarily a cause of concern. It should be noted that the highest deviations reported in intact pelvises were also on the iliac regions [66] indicating that the asymmetry in those regions after reconstruction may have occurred naturally prior to fracture.

The DCMs of some of the subjects, particularly Subject 7, exhibit grey areas (Fig. 4.12 - Fig. 4.14). Grey areas on DCMs could be a result of either one of two things. Either there is no corresponding material on the test surface or the differences between the two surfaces are greater than the upper threshold (6 mm in this case). For Subject 7, there was no corresponding material on the reconstructed side, hence the grey color in the acetabular cup. This may be due to fractured pieces that were too small to be captured by the CT scanner or were lost in the segmentation process in Mimics®.

Another method was tested prior to the automatic symmetric registration method used in this study; it involved manual point-to-point alignment of the fractured pieces (Fig. 4.10). The two methods were performed on Subject 1 to examine the differences. The RMS of deviations and percentage of points within ± 2 mm for the automatic symmetric registration method was 1.39 mm and 89.2% and was 1.62 mm and 80.6% for the manual point-to-point alignment method. These statistics show that the automatic symmetric registration method provides a more symmetric reconstruction. When comparing the DCMs for Subject 1 obtained from each of the methods (Fig. 4.9 and Fig. 4.11), the highest deviations using the automatic method are along the fracture line, while there are much higher deviations in the iliac region of the pelvis that was reconstructed using manual point-to-point alignment (characterized by the areas shown in dark blue and dark red). Reconstructing the pelvis using this method may result in biomechanical differences between the reconstructed and intact sides, since the iliac regions are sites of major muscle attachments. However, future work will be needed to investigate this further. This method also required more use of skill and was more time consuming, so the automatic symmetric registration was the preferred method used in further analysis.

Despite the significance of this study, there are a few limitations. This pelvis reconstruction technique is only applicable for unilaterally fractured pelvises where an intact side is available to serve as a template during the reconstruction procedure. Hence, bilaterally fractured pelvises cannot be reassembled using this technique. It would likely be possible to use the presented technique in bilateral fractures where the fractures on each side do not occur in the same location, however, this approach has not yet been investigated. In addition, our reconstruction method did not incorporate a haptic feedback mechanism as reported in previous studies [10, 44, 63]. This mechanism detects if any of the bone fragments overlap when repositioning them in their assumed locations. However, overlapping pieces are not likely to occur when following the proposed reconstruction method in this paper. This is because the pelvis is symmetric and the fractured hemipelvis is reconstructed according to the intact hemipelvis geometry. Also, the segmentation process in Mimics® creates smoother fracture lines by slightly removing material. This forms a small gap between the fractured pieces when reconstructed, rather than having them overlap. However, this is not expected to affect the results, since the fractured pieces are aligned with the intact side based on hundreds of points outside of the fracture region. The material lost in the

segmentation process is insignificant compared to the remaining volumes and the overall pelvis reduction remains accurate. Finally, this study involved only 5 males and 3 females and, although the present results show no observable differences between them, further investigation with more test subjects would be required to make a more thorough assessment.

The technique used in this study employed automatic symmetric registration of the fractured pelvic pieces by highlighting the corresponding regions on the intact hemipelves and using them as templates. This preserves the natural symmetry of the pelvis, minimizes user subjectivity and is less time consuming than the conventional manual reconstruction procedures. The proposed technique also allows for a more accurate reconstruction of the pelvis and has the potential to help surgeons provide their patients with better treatment plans by assisting them in the surgical planning phase. The final product of this method would be a complete 3D virtual model of a reconstructed pelvis and this would eliminate the need for surgeons to decide where the fractured pieces would need to be relocated in order to restore the pelvis to its original shape.

Future work will aim at developing a method for reconstructing bilaterally fractured pelvises. Three-dimensional models for the average shape of male and female pelvises will be built from a database of various intact pelvises. With these models, the same procedure presented in this work can then be applied to reconstruct bilaterally fractured pelvises.

Chapter 5: Reconstruction for Bilaterally Fractured Pelvises

This chapter will be submitted as a journal article to a peer-reviewed journal.

5.1 Abstract

Pelvic fractures are one of the most severe musculoskeletal injuries and are associated with high rates of mortality and morbidity. With unilateral pelvic fractures, the contralateral hemipelvis can be used as a template in virtual reconstruction, however, this cannot be applied for bilateral fractures. Therefore, in this study, statistical shape modelling was used to build average pelvic shapes that can serve as templates when reconstructing bilaterally fractured pelvises. Four average shape models were created for the male and female, left and right hemipelves using CT scan data of intact pelvises from 20 male and 20 female subjects. These models were used as templates to reconstruct 8 unilaterally fractured pelvises. Deviation analyses between the reconstructed and intact hemipelves had an average root mean square (RMS) of 1.46 ± 0.32 mm, which is less than the 2 mm threshold for causing hip joint complications. The reduction quality was also evaluated by comparing these results with the same pelvises that were reconstructed by using the intact hemipelves as templates. The average RMS in this case was 1.30 ± 0.27 mm, which is close to the average shape reconstruction RMS. This indicates that the reconstructions are reliable and the average shape models can be used to reconstruct bilaterally fractured pelvises. However, the RMS values and the deviation color maps showed that reconstructions are less accurate for fractures in areas that experience a larger variation between subjects, such as the iliac and pubic regions. The proposed technique can potentially provide quick and accurate treatment plans for pelvic fracture patients, which is necessary for recovery.

5.2 Introduction

Pelvic fractures are severe injuries that typically result from blunt high-energy trauma to the pelvic region [67–69], most often due to motor vehicle crashes or falls [70]. Patients with pelvic fractures often sustain additional life-threatening injuries, including pelvic hemorrhages and sepsis [71, 72]. Consequently, fractures in the pelvic bone are associated with high rates of mortality and morbidity [4, 68, 69, 72, 73]. Studies have shown that urgent and accurate reconstruction of these fractures

is necessary, especially in cases where there are further complications, such as soft tissue injuries [6, 17].

Achieving satisfactory reduction of a fractured pelvis depends on the nature of the fracture and its location. Since the pelvis is considerably symmetric about the midsagittal plane [35, 36, 66], this bilateral symmetry can be utilized in virtual pelvis reconstruction. For unilateral pelvic fractures, where only one side of the pelvis is damaged, pelvis reduction can be achieved by using the opposite intact side as a template for the reconstruction. This technique maintains patient-specificity, yields satisfactory results and can reduce the wait-times for patients [46, 74, 75]. However, for bilateral pelvic fractures, where both sides of the pelvis are damaged, there is no viable model to serve as a template for the virtual reconstruction procedure [52].

Virtual pelvis reconstruction is becoming more popular in the surgical planning process, as it has the potential to reduce operation times and provide more accurate reductions, which ultimately decreases the risk for the patients. Therefore, for bilaterally fractured pelvises, we propose an average pelvic shape that could serve as a template for the reconstruction procedure. The proposed method to obtain this average pelvic shape is statistical shape modelling (SSM).

SSM has been growing in popularity in recent years, where models of various bones have been created to improve the design of orthopedic implants, study the effects of bone shape on osteoarthritis and assist in the surgical planning processes [47, 76]. Researchers have also used SSM to accelerate and improve pelvis segmentation processes, particularly in the acetabular area, where traditional segmentation protocols are not always accurate [77, 78]. Previous studies have generated statistical shape models for the pelvis from healthy CT data sets and have shown promising results. The mean distances between these models and sample intact pelvises was calculated to determine whether they can sufficiently represent various pelvis shapes [79, 80]. The clinically acceptable deviation threshold for preventing osteoarthritis in the hip joints is 2 mm [11–16] and this was used as the criteria to evaluate the applicability of these statistical shape models. Results showed that the average of these mean distances was 2 mm or less, indicating that these models can potentially be used in preoperative planning of computer-assisted hip surgeries [79, 80]. Skadlubowicz et al. also developed a pelvis statistical shape model from a pool of 20 CT data sets [52], to find the optimal bone shape for reconstructing the pelvis after bone tumor resection. The statistical shape model was matched to a model of a patient with an ischiopubic rami resection

on the left hemipelvis. The mean difference between the two models was 0.024 mm, suggesting that the statistical shape model is an excellent fit and can be used as a template for oncologic surgical planning [52].

Despite the promising results and applications of SSM, there is limited knowledge in the literature about its performance in unilateral and bilateral pelvic fracture reconstruction. Therefore, the objective of this work was to build an average shape model for the pelvis and assess its applicability in virtual pelvis reconstruction. The average shape models focus on the left and right hip joints, rather than the entire structure of the pelvis (which includes the sacrum). Since this work focuses on fractures in the hip bone, it is important to capture the morphological shape of that bone in itself. Also, the pelvis is a sexually dimorphic structure [81, 82], so separate models were created for the male and female, left and right hemipelves. These models were examined by studying the differences between them and the group of pelvises they were generated from. Finally, the average shape models generated were tested by using them as templates to reconstruct unilaterally fractured pelvises. The results were then be compared with the same pelvises that were reconstructed by using the uninjured sides as templates. A case study for a bilaterally fractured pelvis was also used to demonstrate the reconstruction procedure using the average shape.

5.3 Methods

5.3.1 Developing the Average Pelvic Shape

Computed tomography (CT) images of the pelvic regions of 40 subjects (20 males, 20 females, age range 18-25 years with a mean age of 21.3 years) were used to create the average male and female pelvis shapes. Approval to use this data retrospectively and anonymously was obtained from the Health Research Ethics Board with a waiver of consent. Since these scans were performed for clinical purposes across a health region, the scanners and scanning parameters were not standardized. Siemens, General Electric Medical Systems, Toshiba and Philips scanners were used. The average in-plane pixel length for the images was 0.738 mm (range 0.439–0.928 mm) with a typical resolution of 512×512 pixels per slice. The average slice thickness and number of slices was 1.46 mm (range 1–3 mm) and 347 (range 81–731), respectively.

The scans were digitized into 3D models by importing them into Materialise-Mimics (Materialise®, Leuven, Belgium) and segmenting the pelvic bone using the same procedure in our

previously published work [66]. Once the pelvic bone was isolated from the surrounding soft tissue and bones, each hemipelvis was saved as a separate STL file.

A statistical shape modelling algorithm was developed in Python® (Python Software Foundation, Virginia, USA) and used to build an average shape for the pelvic bone. The algorithm was based on the parallel groupwise registration algorithm developed by Giessen et. al [83]. For the rigid and non-rigid registration tasks, the Coherent Point Drift (CPD) method, developed by Myronenko and Song [84], was employed.

The inputs for the groupwise registration algorithm are the point sets representing the shapes of the hemipelves. The STL files of the hemipelves are first used to extract the locations of the points, i.e. point sets (Fig. 5.1a). Since these point sets ranged from 500,000 to 1,000,000 points, it would have been difficult to perform the matrix operations included in the algorithm. Therefore, a voxel-based sampling algorithm is employed. Each hemipelvis' point set was subsampled to approximately 10,000 points to sufficiently capture the complex geometry, while maintaining reasonable computational effort (Fig. 5.1b). These subsampled point sets were then normalized with respect to translation, scale and rotation (Fig. 5.1c). The normalized point sets then undergo rigid registration, where one of the point sets is considered the target and the rest of the point sets are aligned onto it using the rigid CPD method [84], as shown in Fig. 5.2a. Once this is achieved, the non-rigid registration process begins. In this stage, one of the rigidly aligned point sets is selected as the reference and registered onto the rest of the point sets using the non-rigid CPD method [84], as displayed in Fig. 5.2b. Since all non-rigid registrations originate from the reference point set, it can be claimed that, after the alignments, correspondence is constructed between the point sets (Fig. 5.2c). More specifically, the counterparts of each point of the reference point set on the other point sets is established (Fig. 5.2c). Finally, the average shape is obtained by computing the mean of these registered point sets (Fig. 5.2c).

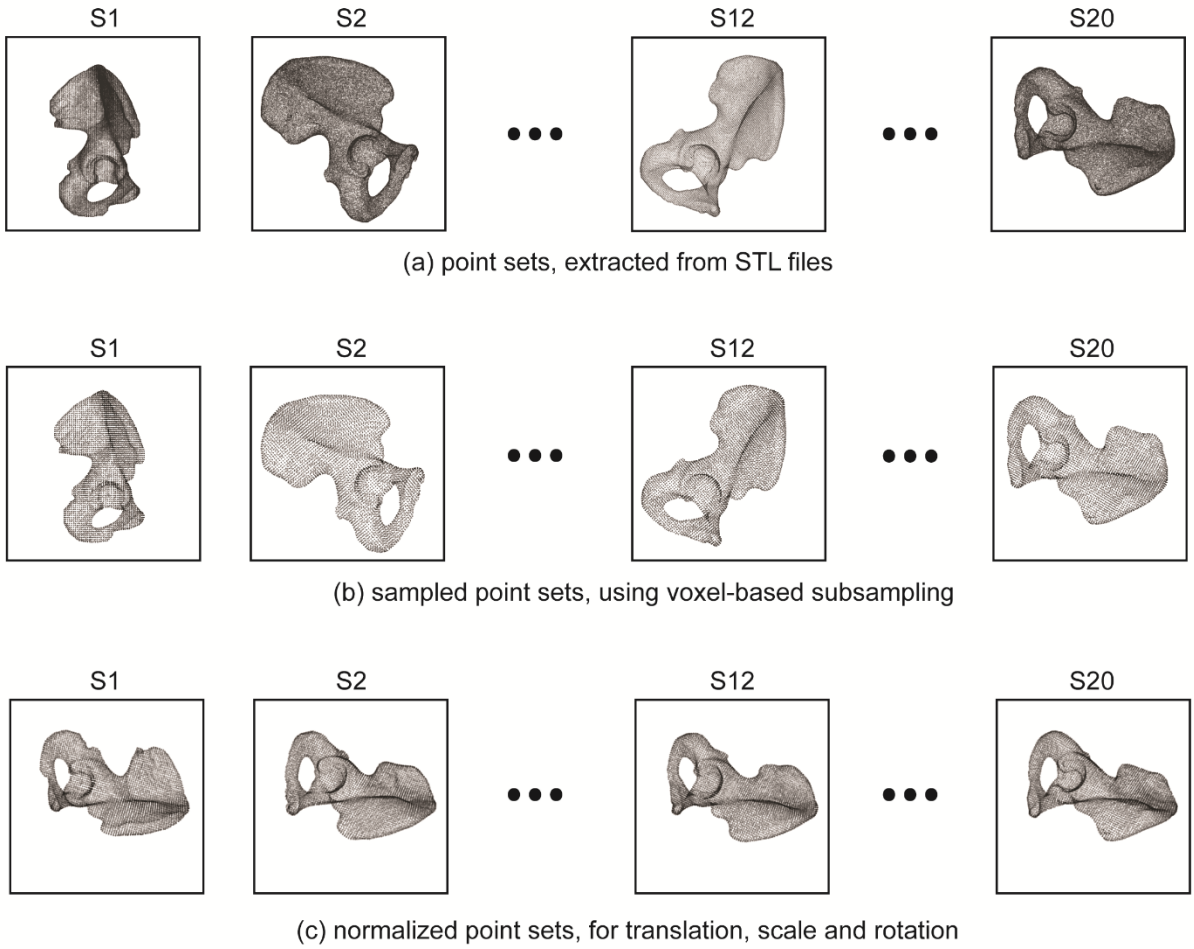

Fig. 5.1 Preprocessing of the point clouds for the male left hemipelves dataset. Subjects 1, 2, 12 and 20 are used to demonstrate the process. (a) The point set data for each hemipelvis is extracted from its respective STL file. (b) The point sets are subsampled to approximately 10,000 points each. (c) The point sets are normalized with respect to translation, scale and rotation.

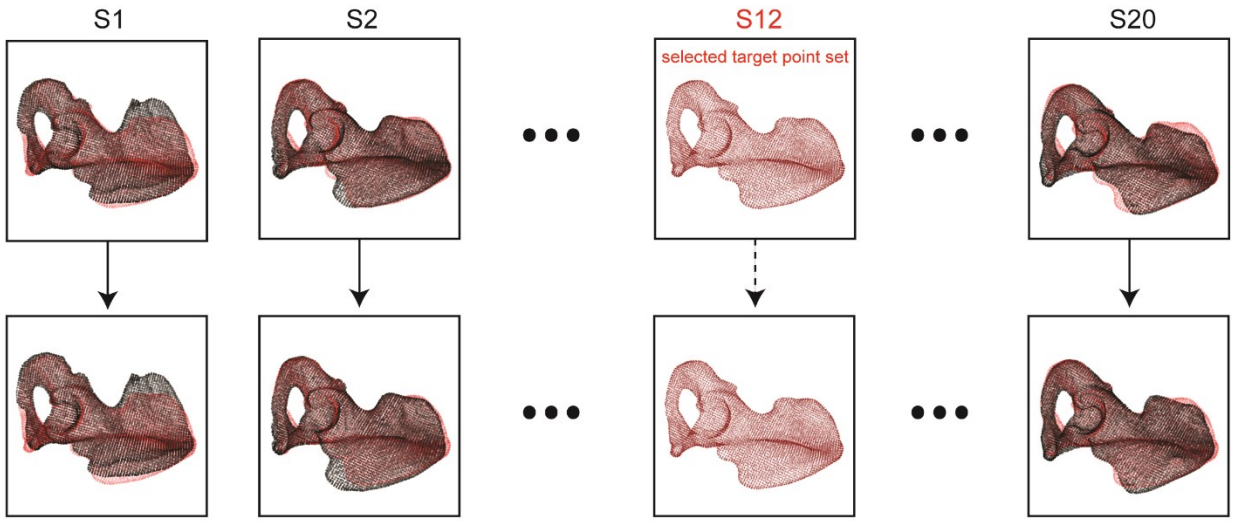

(a) rigid registration of the (normalized) point sets onto the selected point set

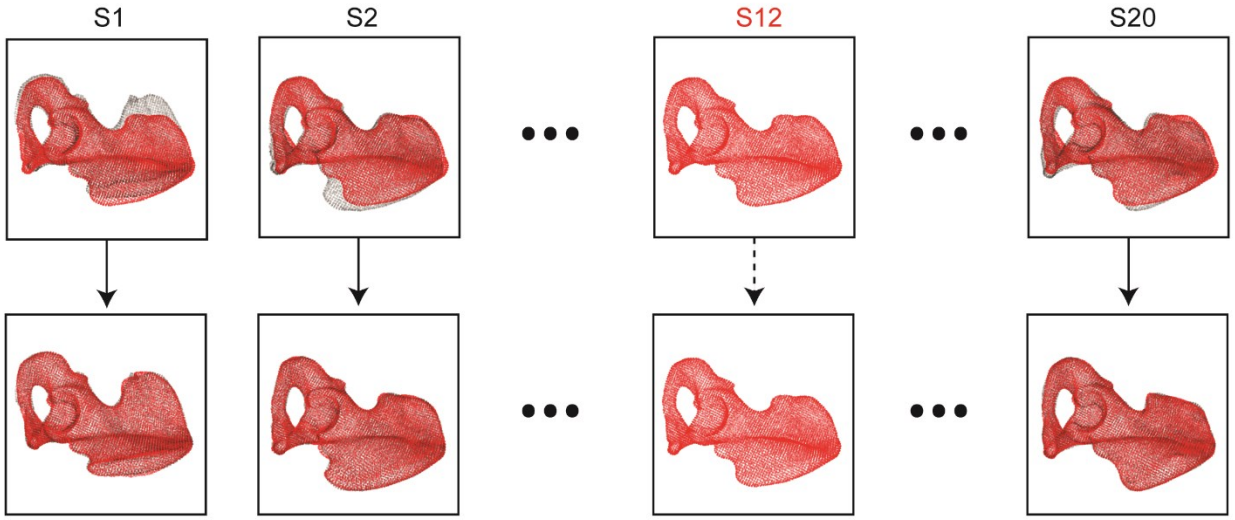

(b) non-rigid registration of the selected point set on the (rigidly-aligned) point sets

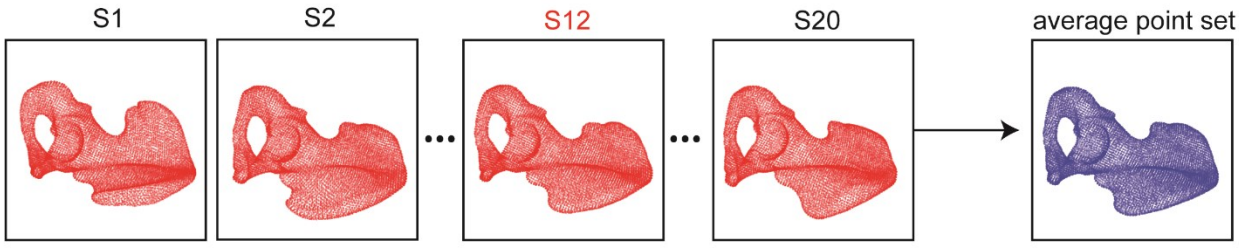

(c) correspondence among the point sets and the average point set

Fig. 5.2 Stages of the groupwise registration process for the male left hemipelves dataset. Subjects 1, 2, 12 and 20 are used to demonstrate the process. (a) Rigid registration of the normalized point sets onto the target point set (S12 in this case). (b) Non-rigid registration of the reference point set (S12 in this case) to each of the rigidly aligned point sets. (c) Point set correspondence is achieved and the average of these registered point sets is calculated.

The groupwise registration process was performed on each set of hemipelves separately, i.e. 20 male left hemipelves, 20 male right hemipelves, 20 female left hemipelves and 20 female right hemipelves. The products were four point sets of the average hemipelvis shapes. These point sets were converted into surface models by wrapping them in Geomagic® Control™ 2014 (3D Systems, South Carolina, USA) and were then saved as STL files. Fig. 5.3 shows the anterior and posterior views of the final four average shape models.

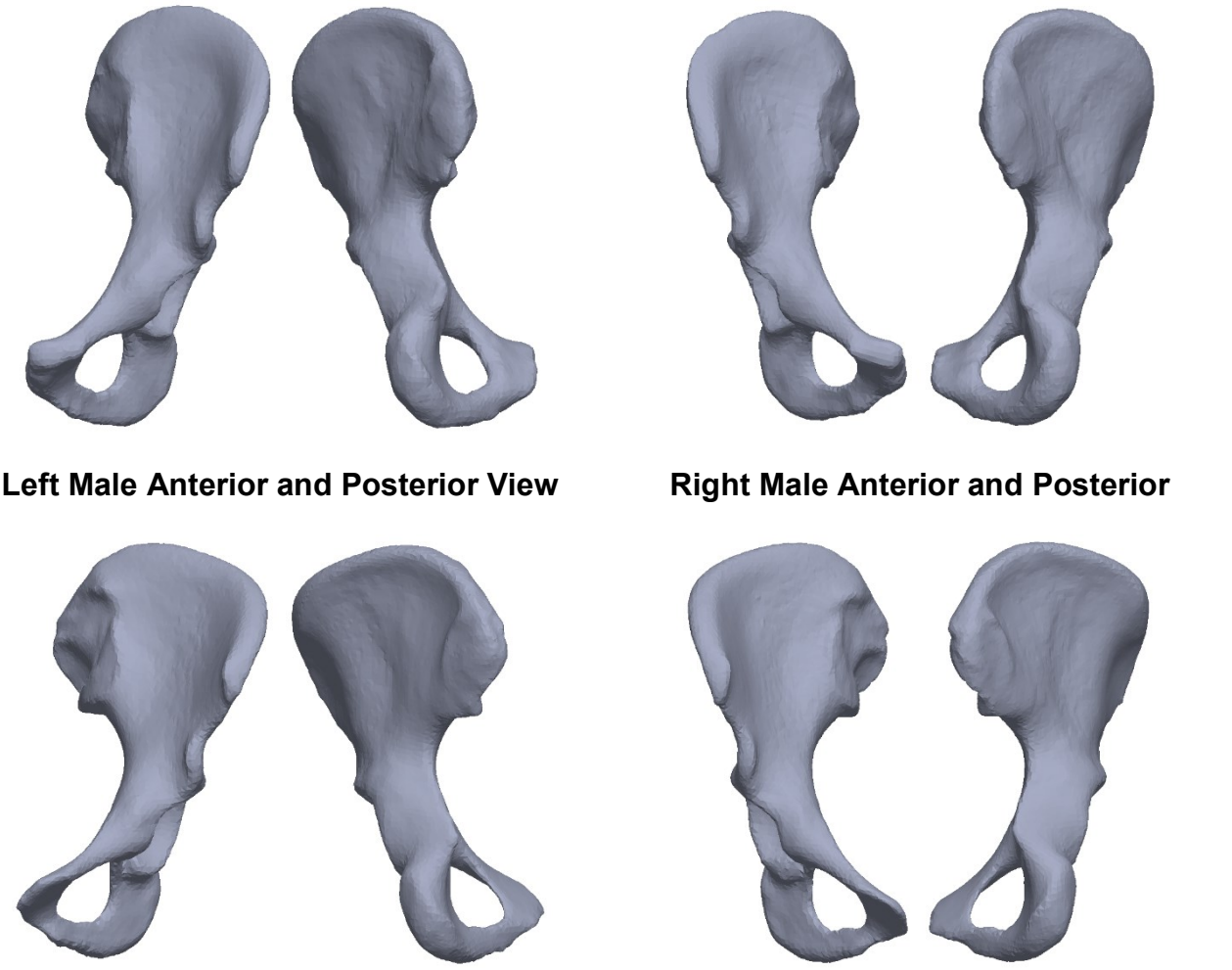

Fig. 5.3 Final average shape models for the left and right sides of the males and females.

The average hemipelvis shapes created can be used to better understand differences in shape between hemipelves. Geometrical deviations between any two surfaces can be determined by performing a 3D deviation analysis in Geomagic®. This provides a deviation color map (DCM), which allows the user to visually analyze the degree of difference between two surfaces by using color. The 3D deviation analysis also provides quantitative data including the root mean square (RMS) of deviations and the percentage of points lying in each subrange of the deviation spectrum. Before conducting the deviation analysis, the hemipelves were first scaled to the same volume as each average hemipelvis shape and then aligned with each other by using the built-in best-fit alignment function of Geomagic®. Deviation analyses were then conducted between each average hemipelvis shape and the respective hemipelves used to create it. The quantitative results were recorded and a few representative DCMs are displayed in the following section. To compare the differences between the male and female average shapes, the male average hemipelvis shapes were first scaled to the same volume as the females. Then 3D deviation analyses were performed between the left female and male average hemipelvis shapes, as well as the right female and male average hemipelvis shapes.

The average hemipelvis shapes were obtained by selecting a random hemipelvis in each group to serve as the initial shape to be deformed. In order to test the sensitivity of the average shape, different hemipelves were chosen as the initial shapes for each group and the RMS between these new average shapes and the corresponding hemipelves was calculated.

5.3.2 Reconstructing Unilateral Pelvic Fractures with the Average Pelvic Shape

The validity and quality of reconstructing fractured hemipelves by using the average hemipelvis shape as a template was evaluated by comparing the results with reconstructions performed by using the mirrored intact hemipelvis as a template. The dataset used here is from a previous study (Chapter 4) and includes 8 patients (5 males, 3 females, age range 20-43 years with a mean age of 29.9 years) with acute unilateral displaced pelvic fractures [75].

The patient CT scans were already digitized into 3D models using Mimics® in Chapter 4. However, in order to use the average hemipelvis shape as a template for rebuilding the fractured hemipelvis, it would need to be scaled to the same volume. Therefore, the cancellous bone area of each of the intact hemipelves was filled in using the segmenting tools in Mimics® to ensure the

correct volume calculation. The intact hemipelvis and each of the fractured pieces were then saved as separate STL files for each subject.

Similar to our previous work, the reconstruction procedure is performed in Geomagic® [75]. The intact hemipelvis, fractured pieces and the corresponding average hemipelvis shape are all imported into the software. The average hemipelvis shape is first scaled to the same volume as the intact hemipelvis, to account for size variations. Each of the fractured pieces are then aligned by highlighting the equivalent region on the average hemipelvis shape to serve as a template. The alignment is accomplished by using the built-in best-fit alignment function of Geomagic®. After aligning all the fractured pieces, this reconstructed hemipelvis is then saved as a new STL file [75].

Reconstruction by using the intact hemipelvis as a template was also performed to provide a means of comparison. The same procedure is followed where the fractured pieces and intact side are imported into Geomagic®. In this case, however, the intact hemipelvis is reflected across the sagittal plane before the alignment procedure. The hemipelvis reconstructed using this method is also saved as a separate STL file [75].

The 3D deviation analyses were performed in Geomagic®, which provided DCMs and quantitative statistics. Deviations within ± 2 mm are deemed sufficient to prevent complications, such as osteoarthritis, in the hip joints [11, 16]. Therefore, the threshold was set at ± 2 mm and was characterized by the green areas of the DCMs. Deviations between ± 2 mm and ± 6 mm were characterized by red/blue regions in the DCMs.

In order to assess the quality of pelvis reduction by using the average hemipelvis shape as a template, various 3D deviation analyses were conducted and the results documented. Since the reflected intact hemipelvis represents the ideal model, we compared (1) the reconstruction using the average shape with the reflected intact side, (2) the reconstruction using the reflected intact side with the reflected intact side, and (3) the two different reconstructions.

5.3.3 Reconstructing Bilateral Pelvic Fractures with the Average Pelvic Shape

A representative example of a patient with a bilaterally fractured pelvis is used to demonstrate the methods applied for virtual reconstruction. The subject is an 18-year-old male and the CT scanner used was a Siemens Definition AS+. The pixel size for the images was 0.494 mm with a resolution

of 650×512 pixels per slice. The slice thickness and number of slices was 1 mm and 419, respectively.

The CT scans were digitized into 3D models using Mimics®, in the same manner as noted previously in Chapter 4. The cancellous bone areas were then filled, in order to scale the average hemipelvis shapes to the equivalent volume. Fig. 5.4 shows the final digitized model completed in Mimics®. The 3D models of all the fractured pieces were then imported into Geomagic® for reconstruction, along with the male average hemipelvis shapes (left and right sides). Each hemipelvis was rebuilt by using its respective average hemipelvis shape as a template and reassembling the pieces in the same manner as previously described in Section 0. A 3D deviation analysis was then conducted between each hemipelvis and its corresponding average shape side to study the quality of the reduction.

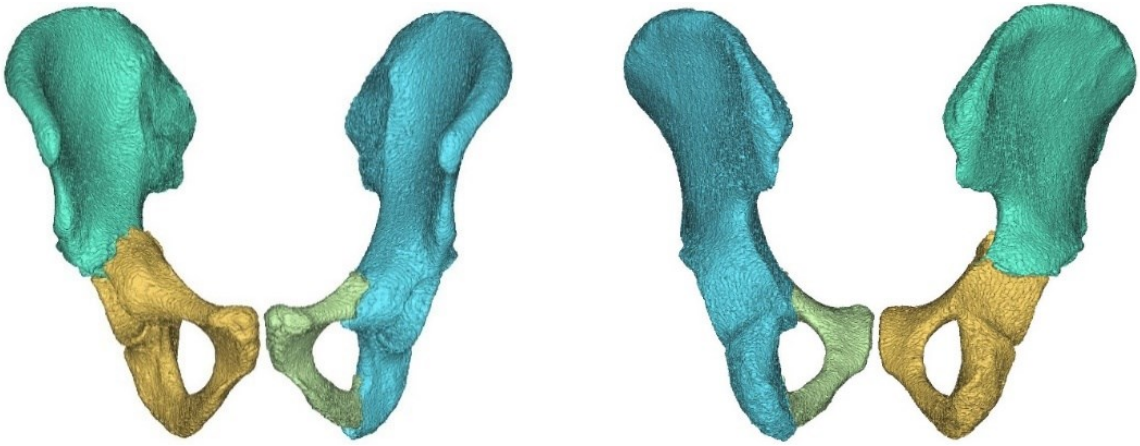

Fig. 5.4 3D model for the bilaterally fractured pelvis created in Mimics® (a) anterior view and (b) posterior view.

5.4 Results

5.4.1 Average Pelvic Shape

5.4.1.1 Deviation Analysis

A summary of the results of the deviation analyses for each of the hemipelvis models with the corresponding average shape model are outlined in Table 5.1. Average values for the RMS and percentage of points within ± 2 mm are presented. DCMs of four subjects from each group are displayed in Fig. 5.5 and Fig. 5.6. The DCMs chosen to display in each group were the subjects with RMS values that are closest to the average RMS. These are representative examples of the mean differences in shape between the subjects and their corresponding average shape models. For the deviation analysis performed between the female and male average hemipelvis shapes, the results are presented in Table 5.2 and the DCMs are displayed in Fig. 5.7.

Table 5.1 Summary of the deviation analysis results for the hemipelvis models with their corresponding average hemipelvis shapes.

3D Deviation Analysis Number	Surfaces		Results	
	Reference Surface	Test Surface	RMS (Average ± SD mm)	Percentage of Points Within ± 2 mm (Average ± SD %)
1	left male average hemipelvis shape	left male intact hemipelvis	2.52 ± 0.69	60.1 ± 11.3
2	right male average hemipelvis shape	right male intact hemipelvis	2.50 ± 0.70	60.6 ± 13.0
3	left female average hemipelvis shape	left female intact hemipelvis	2.39 ± 0.44	62.1 ± 8.64
4	right female average hemipelvis shape	right female intact hemipelvis	2.41 ± 0.42	61.8 ± 8.10

Table 5.2 Deviation analysis results between the male and female average hemipelvis shapes.

3D Deviation Analysis Number	Surfaces		Results	
	Reference Surface	Test Surface	RMS (mm)	Percentage of Points Within ± 2 mm (%)
1	left female average hemipelvis shape	left male average hemipelvis shape	1.97	72.6
2	right female average hemipelvis shape	right male average hemipelvis shape	2.06	68.1

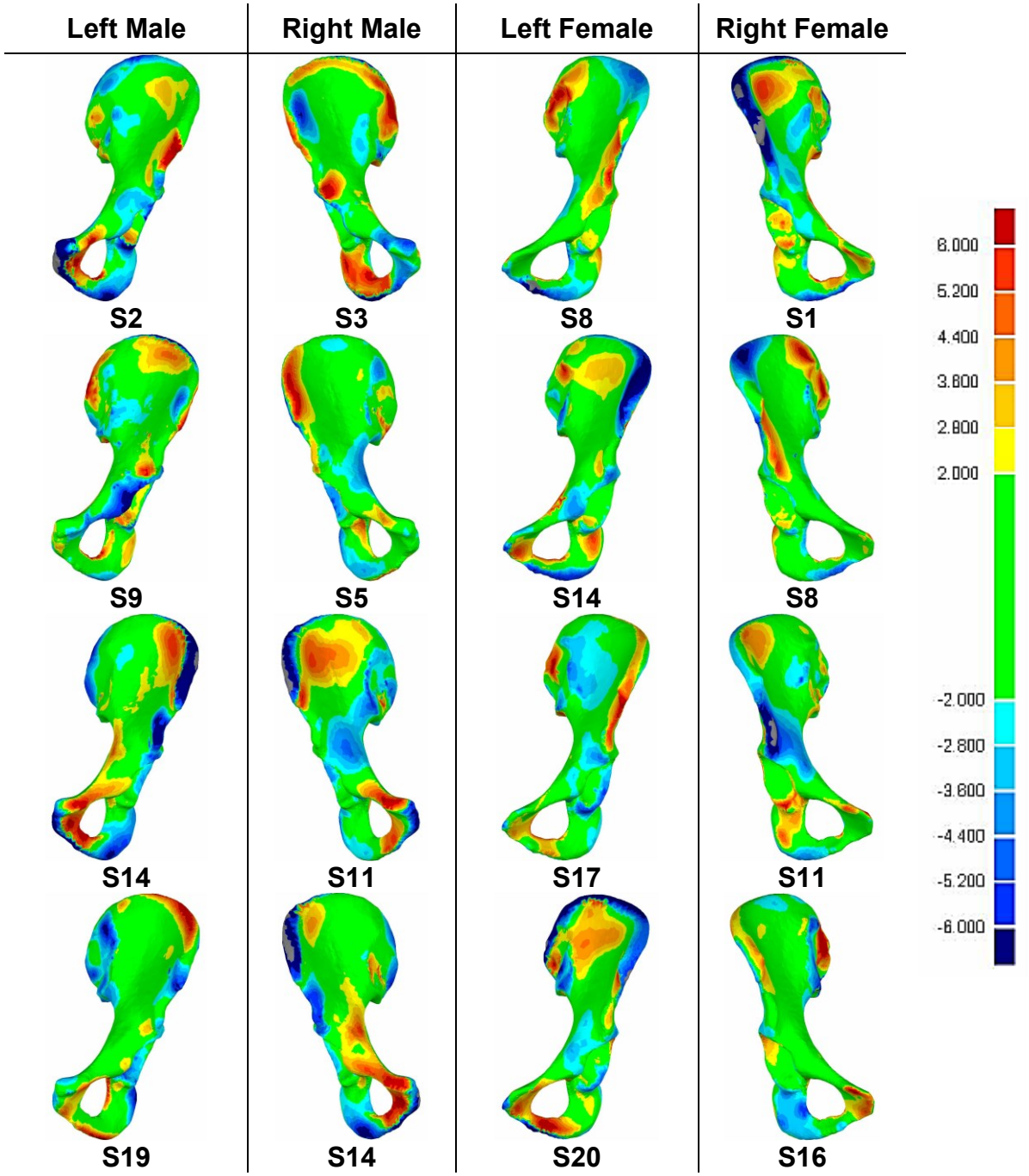

Fig. 5.5 Anterior view deviation color maps (mm) between four example hemipelves and their corresponding average hemipelvis shape.

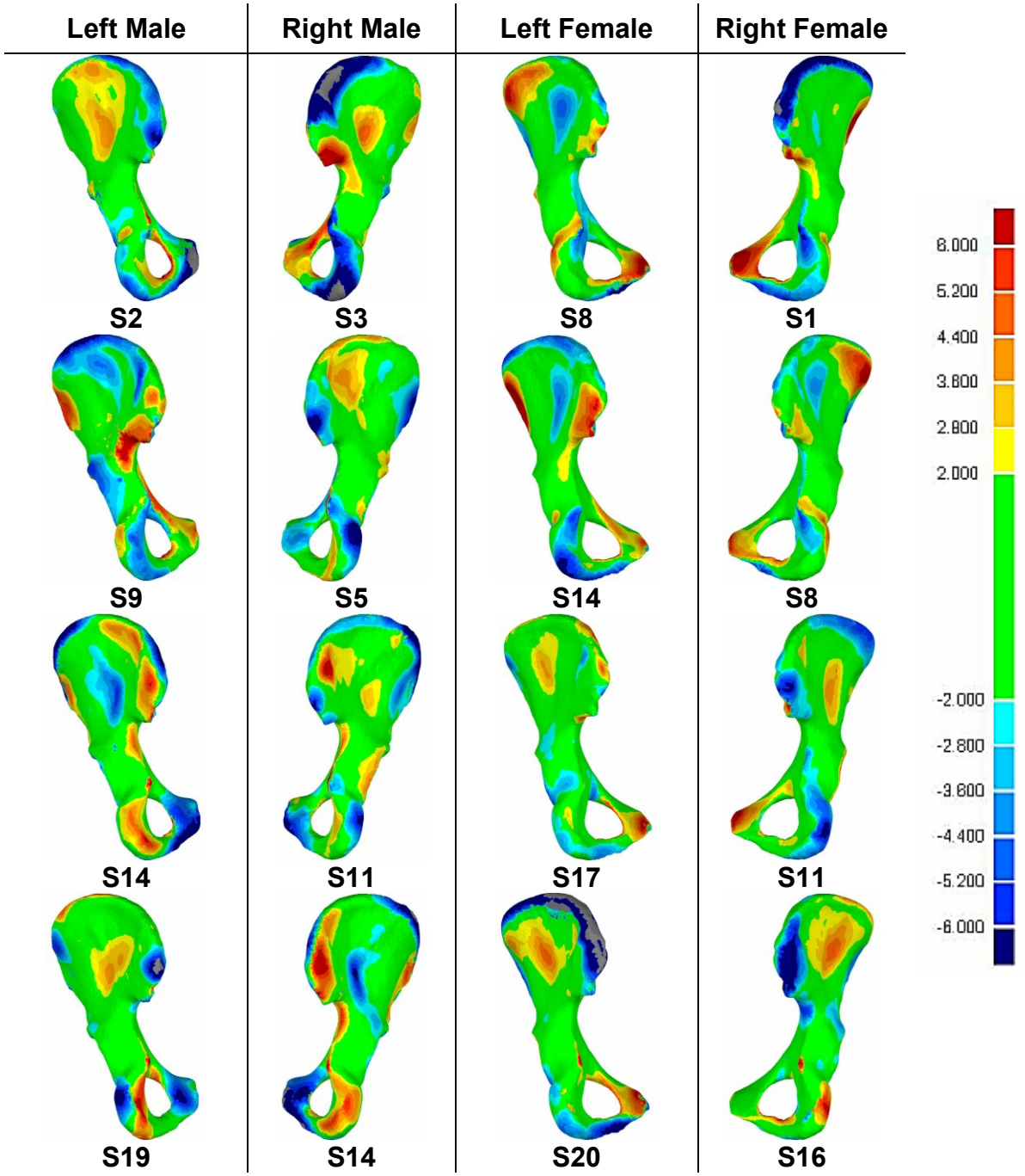

Fig. 5.6 Posterior view deviation color maps (mm) between four example hemipelves and their corresponding average hemipelvis shape.

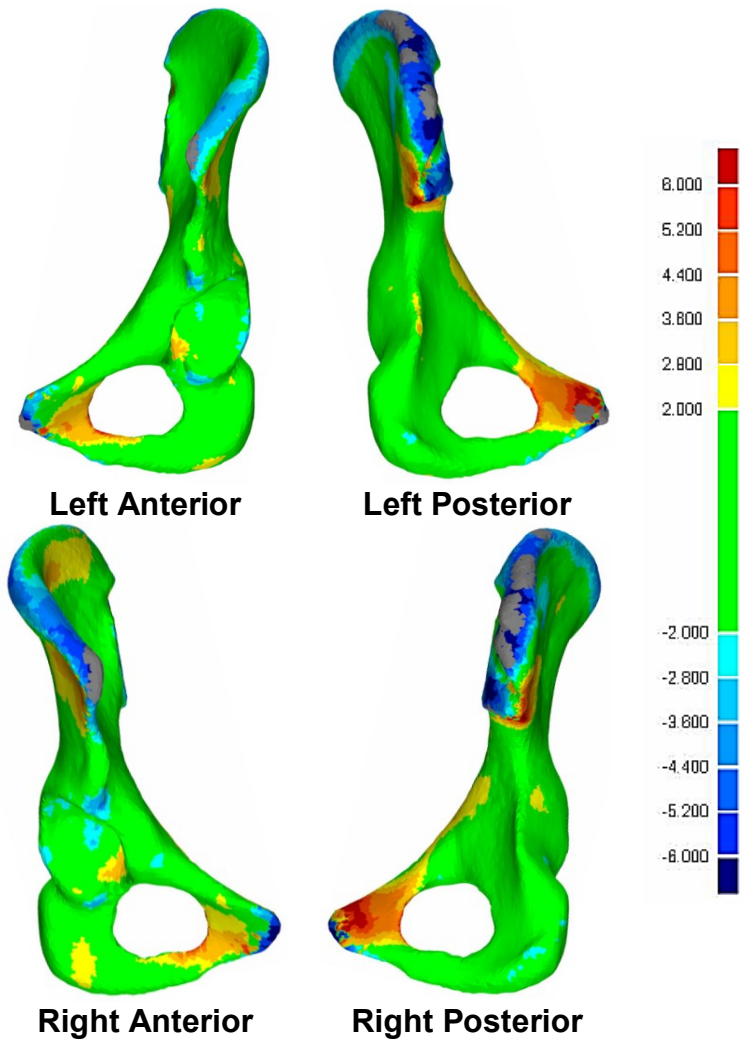

Fig. 5.7 DCMs resulting from the 3D deviation analyses conducted between the left female and male average hemipelvis shapes and the right female and male average hemipelvis shapes.

5.4.1.2 Sensitivity Analysis for Average Pelvic Shape

Different hemipelves for the left side male and female groups were chosen as the initial shapes to test the sensitivity of the average hemipelvis shape. Subjects 4, 3 and 6 were chosen as the initial shapes for the females and subjects 12 and 3 were chosen as the initial shapes for the males. The resulting RMS values of the deviation analyses conducted between each average hemipelvis and the corresponding hemipelves for all runs are displayed in Table 5.3 and Table 5.4.

Table 5.3 Results of the 3D deviation anaylsis conducted between the left female average hemipelvis shapes and the corresponding hemipelves. The initial shapes chosen for these runs were subjects 4, 3 and 6. RMS is the root mean square deviation.

Subject #	S4 as Initial Shape RMS (mm)	S3 as Initial Shape RMS (mm)	S6 as Initial Shape RMS (mm)
S1	2.67	2.21	2.40
S2	1.79	1.82	1.70
S3	3.05	2.45	2.75
S4	1.45	1.72	1.57
S5	2.25	2.01	2.01
S6	3.14	2.68	2.82
S7	2.63	2.72	2.58
S8	2.38	2.26	2.30
S9	2.75	2.96	2.69
S10	1.89	1.73	1.77
S11	1.99	1.91	1.86
S12	2.02	2.05	1.94
S13	2.99	2.70	2.77
S14	2.47	2.20	2.31
S15	2.00	1.77	1.81
S16	2.49	2.45	2.49
S17	2.36	2.32	2.18
S18	2.50	2.59	2.36
S19	2.50	2.44	2.41
S20	2.42	2.05	2.19
Average	2.39	2.25	2.25
SD	0.44	0.37	0.38

Table 5.4 Results of the 3D deviation anaylsis conducted between the left male average hemipelvis shapes and the corresponding hemipelves. The initial shapes chosen for these runs were subjects 12 and 3. RMS is the root mean square deviation.

Subject #	S12 as Initial Shape RMS (mm)	S3 as Initial Shape RMS (mm)
S1	4.66	4.70
S2	2.70	2.66
S3	3.30	3.22
S4	1.99	2.05
S5	1.96	2.14
S6	2.02	1.99
S7	2.03	1.98
S8	3.37	3.35
S9	2.57	2.57
S10	2.82	2.85
S11	2.32	2.29
S12	1.71	1.95
S13	2.33	2.41
S14	2.66	2.75
S15	1.69	1.78
S16	2.19	2.31
S17	3.02	3.14
S18	2.28	2.42
S19	2.58	2.72
S20	2.15	2.20
Average	2.52	2.57
SD	0.69	0.67

5.4.2 Unilateral Pelvic Fractures

The results of the 3D deviation analyses for the unilaterally fractured pelvises are displayed in Table 5.5 - Table 5.7. The RMS of deviations and the percentage of points within the ± 2 mm threshold are recorded. The average values for these parameters were calculated and a summary of the results is shown in Table 5.8. The average RMS and average percentage of points between ± 2 mm was 1.46 ± 0.32 mm and 85.7 ± 6.22 % in the first deviation analysis where the hemipelves were constructed by using the average hemipelvis shape as a template and compared to the reflected intact side. The average RMS and average percentage of points between ± 2 mm was 1.30 ± 0.27 mm and 91.3 ± 2.56 % in the second deviation analysis where the hemipelves were constructed by using the reflected intact hemipelvis as a template and compared to the reflected intact side. The average RMS and average percentage of points between ± 2 mm was 0.66 ± 0.38 mm and 95.8 ± 3.03 % in the third deviation analysis where both reconstructed hemipelves are compared.

It is important to note that the results obtained for subject 5 are not included in the analysis, since it was unable to produce an acceptable reconstruction when the average hemipelvis shape was used as a template. The 3D deviation analysis conducted between the reconstructed hemipelvis and the reflected intact hemipelvis showed that the RMS was 2.77 mm, which is greater than the 2 mm threshold. The percentage of points between ± 2 mm was 56.2 %, which is quite low.

Table 5.5 Results of the 3D deviation analysis conducted between the hemipelvis reconstructed by using the average hemipelvis shape as a template and the intact hemipelvis (reflected across the sagittal plane). RMS is the root mean square deviation.

Subject #	Sex (M/F)	Fracture side (L/R) and location	RMS (mm)	Percentage of points between ± 2 mm (%)
S1	M	L - ilium	1.85	80.9
S2	M	L - acetabulum	1.26	91.1
S3	M	L - acetabulum	1.30	88.9
S4	M	R - acetabulum	1.85	74.7
S6	F	L - pubis	1.44	84.8
S7	M	R - acetabulum	1.54	87.2
S8	F	L - pubis	0.98	92.5
Average			1.46	85.7
SD			0.32	6.22

Table 5.6 Results of the 3D deviation anaylsis conducted between the hemipelvis reconstructed by using the intact hemipelvis as a template and the intact hemipelvis (reflected across the sagittal plane). RMS is the root mean square deviation.

Subject #	Sex (M/F)	Fracture side (L/R) and location	RMS (mm)	Percentage of points between ± 2 mm (%)
S1	M	L - ilium	1.59	90.5
S2	M	L - acetabulum	1.26	91.2
S3	M	L - acetabulum	1.24	89.2
S4	M	R - acetabulum	1.56	90.3
S6	F	L - pubis	1.12	93.4
S7	M	R - acetabulum	1.51	88.7
S8	F	L - pubis	0.84	96.0
Average			1.30	91.3
SD			0.27	2.56

Table 5.7 Results of the 3D deviation analysis conducted between the hemipelvis reconstructed by using the average hemipelvis shape as a template and the hemipelvis reconstructed by using the intact hemipelvis (reflected across the sagittal plane) as a template. RMS is the root mean square deviation.

Subject #	Sex (M/F)	Fracture side (L/R) and location	RMS (mm)	Percentage of points between ± 2 mm (%)
S1	M	L - ilium	1.04	94.2
S2	M	L - acetabulum	0.13	99.8
S3	M	L - acetabulum	0.30	98.0
S4	M	R - acetabulum	1.13	90.6
S6	F	L - pubis	0.92	94.5
S7	M	R - acetabulum	0.46	97.4
S8	F	L - pubis	0.61	96.1
Average			0.66	95.8
SD			0.38	3.03

Table 5.8 Summary of the deviation analysis results for the unilaterally fractured pelvises.

3D Deviation Analysis Number	Surfaces		Results	
	Reference Surface	**Test Surface**	**RMS (Average ± SD mm)**	**Percentage of Points Within ± 2 mm (Average ± SD %)**
1	intact hemipelvis reflected across the sagittal plane	reconstructed hemipelvis by using average hemipelvis shape as a template	1.46 ± 0.32	85.7 ± 6.22
2	intact hemipelvis reflected across the sagittal plane	reconstructed hemipelvis by using intact hemipelvis as a template	1.30 ± 0.27	91.3 ± 2.56
3	reconstructed hemipelvis by using intact hemipelvis as a template	reconstructed hemipelvis by using average hemipelvis shape as a template	0.66 ± 0.38	95.8 ± 3.03

The DCMs of all subjects resulting from the three deviation analyses conducted are displayed in Fig. 5.8 - Fig. 5.10. The green areas of the DCMs are regions with small deviations (< 2 mm), whereas the red/blue areas are regions with high deviations (> 2 mm). It should be noted that positive deviations indicate that the test surface is above the reference surface and vice versa for negative deviations. The DCMs in Fig. 5.8 - Fig. 5.10 may have some grey regions, particularly subjects 1 and 7. These grey regions could mean that there were no corresponding points on the test surface to compare the reference surface to or that the test points are farther than a 6 mm radius.

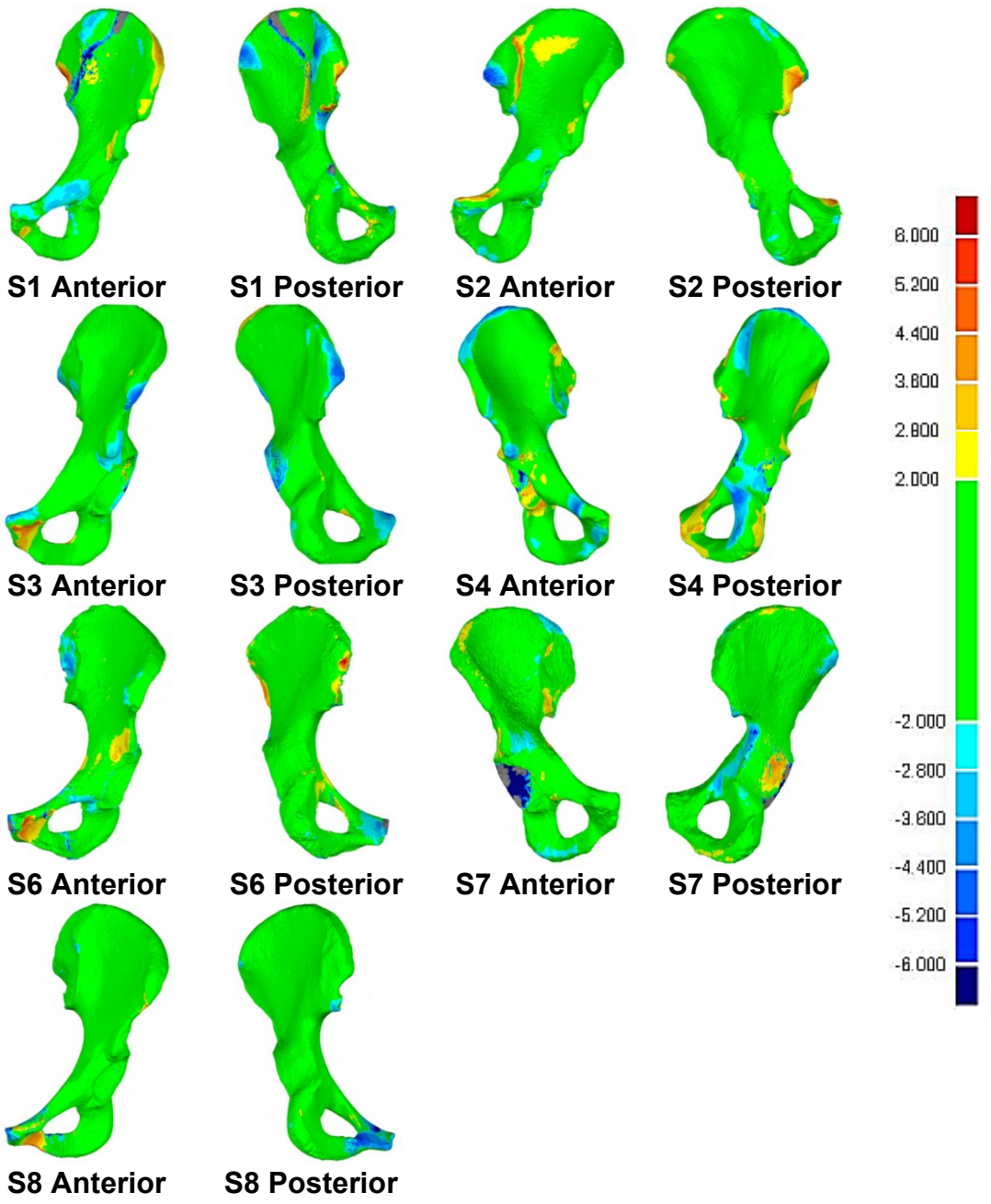

Fig. 5.8 DCMs resulting from the 3D deviation analysis conducted between the hemipelvis reconstructed by using the average hemipelvis shape as a template and the intact hemipelvis (reflected across the sagittal plane).

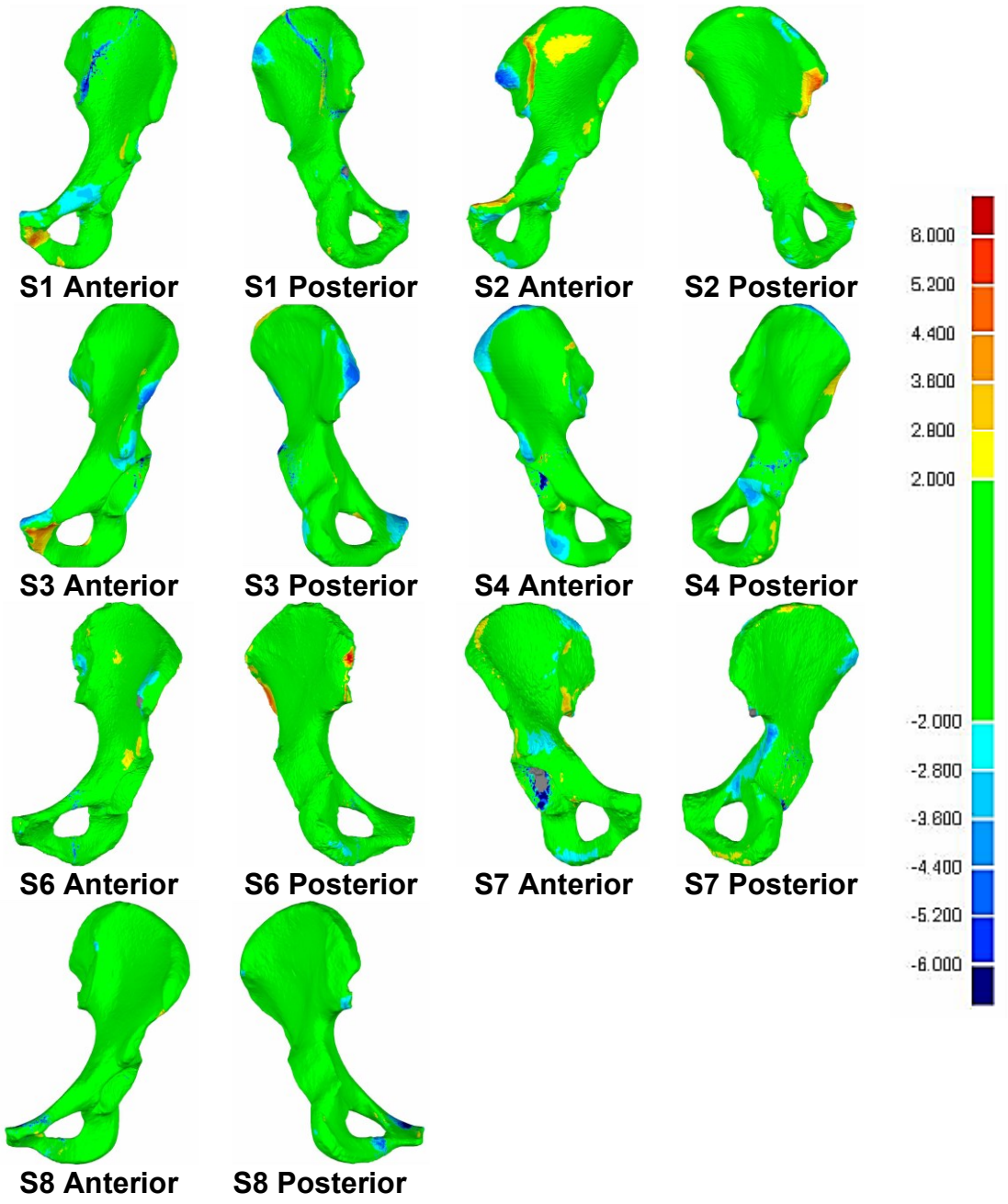

Fig. 5.9 DCMs resulting from the 3D deviation analysis conducted between the hemipelvis reconstructed by using the intact hemipelvis as a template and the intact hemipelvis (reflected across the sagittal plane).

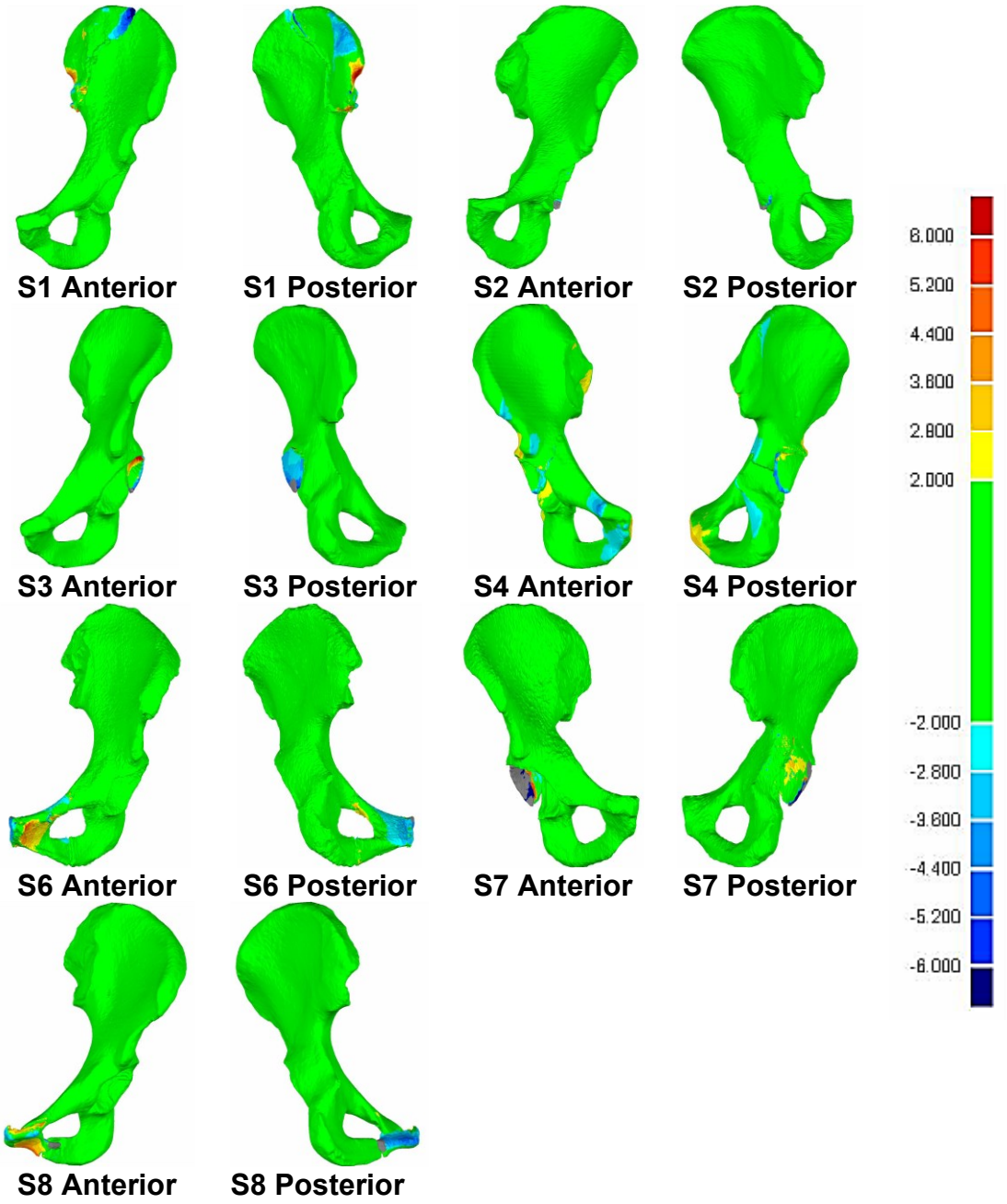

Fig. 5.10 DCMs resulting from the 3D deviation analysis conducted between the hemipelvis reconstructed by using the average hemipelvis shape as a template and the hemipelvis reconstructed by using the intact hemipelvis (reflected across the sagittal plane) as a template.

5.4.3 Bilateral Pelvic Fractures

For the bilaterally fractured pelvis, the deviation analysis between the reconstructed left side and average hemipelvis shape produced an RMS of 2.71 mm and a percentage of points between ± 2 mm of 53.2%. For the reconstructed right side, the RMS was 2.42 mm and the percentage of points between ± 2 mm was 60.4%. The DCMs for these two deviation analyses are displayed in Fig. 5.11.

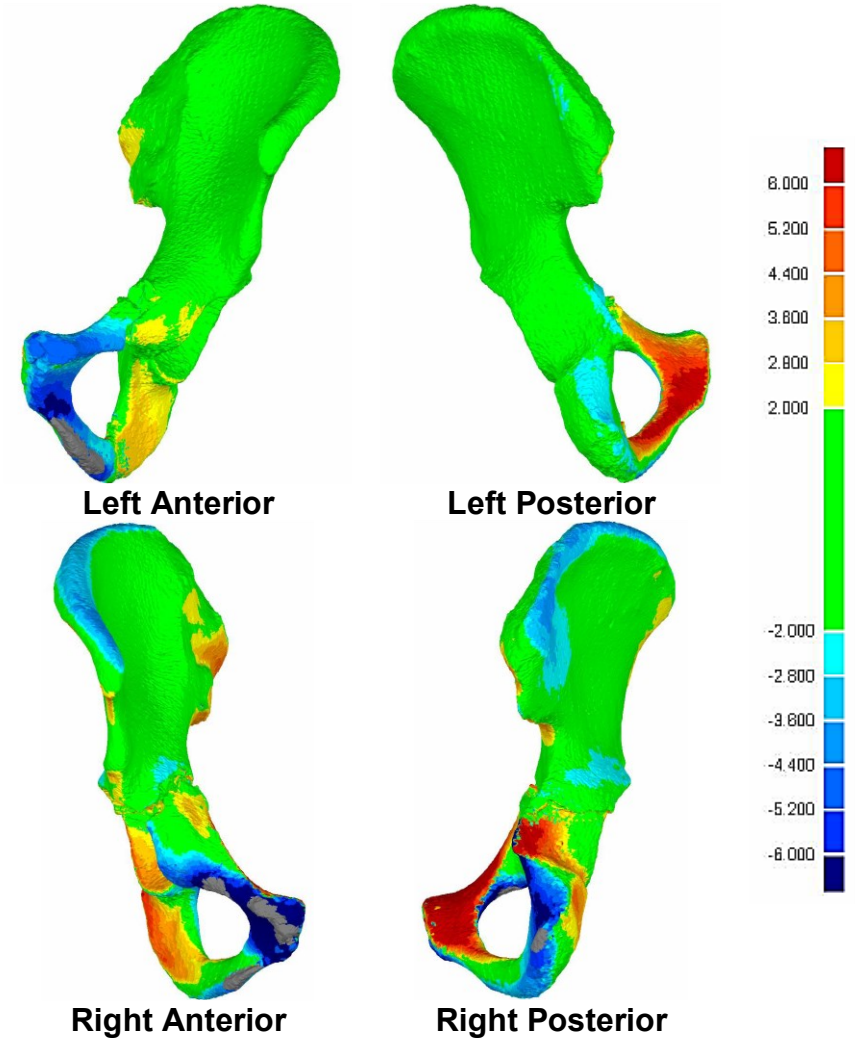

Fig. 5.11 DCMs resulting from the 3D deviation analyses conducted between each side of the bilaterally fractured pelvis and the respective male average hemipelvis shape.

5.5 Discussion

Virtual pelvis reduction has proven to be a useful tool for surgeons in the planning phase of surgery. It has the potential to reduce operation times, while providing accurate reconstructions, which is vital for proper patient recovery [17]. For unilateral pelvic fractures, the virtual reconstruction can be accomplished by mirroring the intact hemipelvis across the sagittal plane and using it as a template. However, this procedure cannot be applied for bilateral fractures, since both hemipelves are injured. Therefore, we built average pelvic shape models using SSM to be utilized for bilateral fracture reconstruction.

Separate average hemipelvis shape models were created for the males and females, since the pelvis varies in shape between the two groups. In total, there were 4 groups, left male hemipelves, right male hemipelves, left female hemipelves and right female hemipelves. Deviation analyses were conducted on Geomagic® between the subjects in each group and their respective average shape, to study the differences. Based on the RMS values and the percentage of points between ± 2 mm (Table 5.1), there were no substantial differences between the left and right sides of both the male and female groups. This further supports the conclusion made in our previous work [66], that the pelvis is considered to be a bilaterally symmetric structure. The DCMs in Fig. 5.5 and Fig. 5.6 show that there are generally higher deviations in the upper parts of the ilia, as well as the ischium and pubis (characterized by the dark blue/red areas), in regions of multiple large muscle attachments. The middle and lower parts of the ilia have lower deviations (characterized by the green areas). This suggests that there are notable variations in shape and pelvic opening within and between the male and female groups, which aligns with previous studies [85–87].

The areas with higher deviations in the DCMs tend to be more variable between people. For fractures in these regions, a subject-specific model would be more desirable for the reconstruction. Though, these areas (iliac wing, ischium and pubis) are non-articular surfaces of the pelvises, so minor variations in these regions after reconstruction are clinically unimportant, as opposed to small variations in the acetabular region which can lead to rapid arthritis. The areas that tend to have lower deviations suggest that these regions have less variability between people. For fractures in these regions, an average shape model may provide reconstructions closer to the subject-specific models.

The final male and female average hemipelvis shapes were compared by conducting deviation analyses between the left male and female hemipelves and the right male and female hemipelves. Results are displayed in Table 5.2. The RMS of the left and right hemipelves was 1.97 mm and 2.06 mm, respectively. The percentage of points between ± 2 mm for the left and right hemipelves was 72.6% and 68.1%, respectively. These differences are expected to be even larger when comparing the entire structure of the pelvis, since there significant differences in shape and pelvic opening between the males and females [81, 82]. The DCMs of Fig. 5.7 showed that there are largest deviations on the iliac crests and pubis regions. This allows us to confirm that the pelvis is a sexually dimorphic structure, as stated in the literature [81, 82] and highlights the importance of creating separate models for the males and females.

In order to build the average pelvis shapes using SSM, one of the subjects in each group must be chosen as the initial shape to be deformed. A sensitivity analysis was conducted to study the effect of choosing different initial shapes on the final average hemipelvis models. For the females, subjects 4, 3 and 6 were chosen as the initial shapes and 3D deviation analyses were performed. The RMS values in Table 5.3 showed that the closest subject to the mean shape was subject 4 in all three tests. Also, the deviations between each of the subjects and the mean shape were consistently high or low for the three cases. In addition, there were no significant differences in the average RMS between the tests. The same conclusion was reached for the males, where subjects 12 and 3 were chosen as the initial shapes (Table 5.4). Subject 15 was the closest to the mean shape in both tests. These results suggest that the final average shape models are insensitive to the choice of the initial shape and provides confidence in the models created.

After obtaining these average hemipelvis shapes, they were used as templates for reconstructing unilaterally fractured pelvises. Deviation analyses were conducted to compare these reductions with ones that were performed by using the reflected intact hemipelves as templates, since these were established to be effective reconstructions [46, 74, 75]. Table 5.8 shows a summary of the quantitative results. The average RMS was close in deviation analysis 1 and 2, 1.46 ± 0.32 mm and 1.30 ± 0.27 mm, respectively. This suggests that the reconstructions based on the average shape were successful. In addition, all subjects in deviation analysis 1 had an RMS less than the 2 mm threshold (Table 5.5), which is necessary to prevent future complications in the hip joints. The average percentage of points between ± 2 mm was higher for deviation analysis 2 (91.3 ± 2.56 %)

than for deviation analysis 1 (85.7 ± 6.22 %). This is to be expected, because the patient's own reflected hemipelvis is likely to be a better representation of their geometry than an average shape template. However, the percentage of points between ± 2 mm for deviation analysis 1 is still considered to be quite high. Based on the DCMs in Fig. 5.8 and Fig. 5.9, the majority of points lying outside the ± 2 mm range (yellow-red and cyan-blue regions) are on the fracture lines and non-articular surfaces of the pelvis, such as the iliac crest. High deviations in the non-articular surfaces are not likely to cause concern and could be attributed to natural asymmetry in those regions, prior to fracture.

Deviation analysis 3 allowed for a direct comparison between both reconstructions. Table 5.7 shows that subjects 1, 4 and 6 have the highest differences between both reconstructions. Subject 1 had an iliac fracture, subject 4 had two acetabular fractures and subject 6 had a pubic fracture (Fig. 4.5). This could suggest that reconstructions based on the average pelvic shapes are less accurate for fractures in the iliac and pubic regions, as well as fractures that split the hemipelvis into more than two pieces. This conclusion aligns with the findings reported above showing that the largest differences between the average shape models and their subjects are in the ilia and inferior regions of the pelvis.

The results of the reconstruction procedure for subject 5 were excluded from the analysis. This subject had an iliac and pubic fracture which split the hemipelvis into three pieces (Fig. 4.5). The reason for exclusion was that the RMS of deviations was 2.77 mm, which is greater than the 2 mm threshold. In addition, the percentage of points between ± 2 mm was 56.2 %, which is quite low compared to the other subjects which had an average of 85.7 ± 6.22 %. This could be attributed to the complex fractures in regions that have been shown to have larger variations between people. In particularly complex fractures, a higher RMS value may still be acceptable for a reconstruction with this technique that may still be more anatomic than having no reconstruction available at all.

The bilaterally fractured pelvis presented in Fig. 5.4 had a pubic fracture on the left hemipelvis and an acetabular fracture on the right hemipelvis. It was reconstructed by using the left and right male average hemipelvis shapes as templates. Results showed that the reconstructed right side was closer to the average shape than the reconstructed left side. This again may suggest that reconstructions based on the average shape for pubic fractures are less accurate than other reconstructions, due to shape variations between subjects in these areas.

To summarize, reconstructions based on the average pelvis shape are generally effective, however, they are less accurate for fractures in regions which exhibit relatively large variations between subjects, such as the ilium and pubis. Future work will aim to combat this issue by creating subgroups for male and female pelvises which are divided based on differences in shape. The fractured pelvis can then be appropriately matched to its respective subgroup average shape for reconstruction. In addition, twenty subjects were used in this study to build the average pelvis shapes; a larger number of test subjects would be more representative of the population and is essential for capturing the differences. Finally, more cases of bilaterally fractured pelvises would need to be tested, in order to provide an informed decision about the viability of the proposed technique.

Virtual pelvic fracture reconstruction has the potential to reduce wait times and operation times, thereby reducing the risk on the patients. Building average pelvis shapes using statistical shape modelling can provide viable templates for virtual reduction of bilaterally fractured pelvises.

Chapter 6: Conclusion

Pelvic fractures are complex injuries which require urgent treatment and accurate reconstructions to minimize the risk on the patient. Recent studies have resorted to the use of virtual pelvic reconstruction techniques in preoperative surgical planning, with the goal of reducing wait times for patients and offering more accurate reconstructions. Despite the notable efforts, current practices require the presence of expert medical professionals, which may be limited. In addition, they are prone to user subjectivity and do not refer to the patients' intact hemipelvis (if present) when performing the reconstruction. This can affect the quality of the reduction since the patients' natural pelvis geometry is not preserved. This thesis aimed to tackle the limitations of current virtual reconstruction techniques.

First, pelvic symmetry was investigated to determine whether the contralateral intact side can be used as a template for unilateral pelvic fracture reconstruction. Fourteen intact pelvises were included in this study and results showed that the pelvis is quite symmetric about the sagittal plane. The average difference between the left and right sides was 1.14 ± 0.26 mm. The highest deviations were found on the non-articular surfaces, particularly major muscle attachment sites. This could be attributed to differences in muscle activation between the left and right sides.

Since the pelvis was established to be sufficiently symmetric, the second stage of this thesis was to develop a technique for virtually reconstructing unilaterally fractured pelvises by using the intact hemipelves as templates. The intact pelvises were reflected across the sagittal plane and the fractured pieces were aligned with it to form a reconstructed hemipelvis. The average difference between the reconstructed hemipelves and their corresponding intact ones was 1.32 ± 0.22 mm, with the largest deviations present along the fracture lines. This result for the mean difference was close to that of the intact pelvises in the symmetry study, which allows us to confirm the validity of this reconstruction technique. Additionally, the method presented here has minimal user subjectivity, preserves the symmetric nature of the pelvis and is less time consuming than manual techniques.

The last stage of this thesis was to introduce a method for virtually reconstructing bilaterally fractured pelvises where there is not intact hemipelvis to serve as a template for the reconstruction. Statistical shape modelling was used to generate an average pelvis shape that can be used as a

template in this procedure. Average shapes were developed for the male and female left and right hemipelves separately using a database of 40 intact pelvises (20 male and 20 female). These average shapes were used to reconstruct the unilaterally fractured pelvises in order to compare the results with the same pelvises that were reconstructed by using their corresponding intact sides. The mean difference for the hemipelves that were reconstructed based on the average shape was 1.46 ± 0.32 mm, which is nearly the same as the pelvises that were reconstructed based on the intact sides. The mean difference between both reconstructed hemipelves (from the average shape and from the reflected intact side) was 0.66 ± 0.38 mm. This suggests that the proposed method can be implemented on bilaterally fractured pelvises. A representative example of a bilaterally fractured pelvis was presented in this work to demonstrate the virtual reconstruction procedure.

Despite the promising results presented in this thesis, there is room for improvement. Future work will aim at using a larger database of pelvises to create the average shape in order to capture the variabilities in the population. In addition, the average shapes will be categorized into several subgroups within the population. This can potentially improve the accuracy of reconstructions for pelvises fractured in regions which display large variations between subjects. Also, regional specific pelvic symmetry will be examined over a larger database of subjects to develop a better understanding of the population differences in those areas, particularly the articular surfaces.

References

1. Ismail HD, Lubis MF, Djaja YP (2016) The Outcome of Complex Pelvic Fracture after Internal Fixation Surgery. Malaysian Orthop J 10:16–21. https://doi.org/10.5704/MOJ.1603.004

2. Schmal H, Markmiller M, Mehlhorn AT, Sudkamp NP (2005) Epidemiology and outcome of complex pelvic injury. Acta Orthop Belg 71:41–47

3. Heetveld MJ, Harris I, Schlaphoff G, Balogh Z, D'Amours SK, Sugrue M (2004) Hemodynamically unstable pelvic fractures: Recent care and new guidelines. World J. Surg. 28:904–909

4. Chong KH, DeCoster T, Osler T, Robinson B (1997) Pelvic fractures and mortality. Iowa Orthop J 17:110–114

5. Dechert TA, Duane TM, Frykberg BP, Aboutanos MB, Malhotra AK, Ivatury RR (2009) Elderly patients with pelvic fracture: Interventions and outcomes. Am Surg 75:291–295. https://doi.org/10.1177/000313480907500405

6. Taller S, Lukás R, Srám J, Krivohlávek M (2005) Urgent management of the complex pelvic fractures. Rozhl Chir 84:83–87

7. Comstock CP, Van Der Meulen MCH, Goodman SB (1996) Biomechanical Comparison of Posterior Internal Fixation Techniques for Unstable Pelvic Fractures. J Orthop Trauma 10:517–522. https://doi.org/10.1097/00005131-199611000-00001

8. (UK) NCGC (2016) Fractures (Complex): Assessment and Management. National Institute for Health and Care Excellence (UK)

9. Nieminen J, Pakarinen TK, Laitinen M (2013) Orthopaedic reconstruction of complex pelvic bone defects. evaluation of various treatment methods. Scand J Surg 102:36–41. https://doi.org/10.1177/145749691310200108

10. Fornaro J, Keel M, Harders M, Marincek B, Székely G, Frauenfelder T (2010) An interactive surgical planning tool for acetabular fractures: Initial results. J Orthop Surg Res 5:1–9. https://doi.org/10.1186/1749-799X-5-50

11. Boudissa M, Courvoisier A, Chabanas M, Tonetti J (2018) Computer assisted surgery in preoperative planning of acetabular fracture surgery: state of the art. Expert Rev Med Devices 15:81–89. https://doi.org/10.1080/17434440.2017.1413347

12. Matta JM, Merritt PO (1988) Displaced acetabular fractures. Clin. Orthop. Relat. Res. 83–97

13. Petsatodis G, Antonarakos P, Chalidis B, Papadopoulos P, Christoforidis J, Pournaras J (2007) Surgically treated acetabular fractures via a single posterior approach with a follow-up of 2-10 years. Injury 38:334–343. https://doi.org/10.1016/j.injury.2006.09.017

14. Elmadag M, Guzel Y, Aksoy Y, Arazi M (2016) Surgical treatment of displaced acetabular fractures using a modified stoppa approach. Orthopedics 39:e340–e345. https://doi.org/10.3928/01477447-20160222-07

15. Kreder HJ, Rozen N, Borkhoff CM, Laflamme YG, McKee MD, Schemitsch EH, Stephen DJG (2006) Determinants of functional outcome after simple and complex acetabular fractures involving the posterior wall. J Bone Jt Surg - Ser B 88:776–782. https://doi.org/10.1302/0301-620X.88B6.17342

16. Letournel E, Judet R (1993) Fractures of the Acetabulum. Springer Berlin Heidelberg, Berlin, Heidelberg

17. Huittinen VM, Slätis P (1973) Postmortem angiography and dissection of the hypogastric artery in pelvic fractures. Surgery 73:454–462. https://doi.org/10.5555/uri:pii:0039606073903164

18. Zeng C, Xing W, Wu Z, Huang H, Huang W (2016) A combination of three-dimensional printing and computer-assisted virtual surgical procedure for preoperative planning of acetabular fracture reduction. Injury 47:2223–2227. https://doi.org/10.1016/j.injury.2016.03.015

19. OpenStax (2013) Anatomy and physiology. OpenStax

20. Pereira G, Paschos NK, Kelly JD (2019) Pelvis and Hip. In: General Orthopaedics and Basic Science. Springer, Cham, pp 9–15

21. Cappozzo A, Catani F, Della Croce U, Leardini A (1995) Position and orientation in space

of bones during movement: anatomical frame definition and determination. Clin Biomech 10:171–178. https://doi.org/10.1016/0268-0033(95)91394-T

22. Khurana B, Sheehan SE, Sodickson AD, Weaver MJ (2014) Pelvic ring fractures: What the orthopedic surgeon wants to know. Radiographics 34:1317–1333. https://doi.org/10.1148/rg.345135113

23. Tile, Marvin, Helfet, David L., Kellam JF (2015) Fractures of the Pelvis and Acetabulum. Georg Thieme Verlag, Stuttgart

24. Pennal GF, Tile M, Waddell JP, Garside H (1980) Pelvic disruption: assessment and classification. Clin Orthop Relat Res 12–21. https://doi.org/10.1055/s-2008-1038277

25. Burgess AR, Eastridge BJ, Young JWR, Ellison TS, Ellison PS, Poka A, Bathon GH, Brumback RJ (1990) Pelvic ring disruptions: Effective classification system and treatment protocols. J Trauma - Inj Infect Crit Care 30:848–856. https://doi.org/10.1097/00005373-199007000-00015

26. Young JWR, Burgess AR, Brumback RJ, Poka A (1986) Pelvic fractures: Value of plain radiography in early assessment and management. Radiology 160:445–451. https://doi.org/10.1148/radiology.160.2.3726125

27. Islam K, Dobbe A, Komeili A, Duke K, El-Rich M, Dhillon S, Adeeb S, Jomha NM (2014) Symmetry analysis of talus bone. Bone Joint Res 3:139–145. https://doi.org/10.1302/2046-3758.35.2000264

28. Baclig MM, Westover L, Adeeb S (2019) Categorizing three-dimensional symmetry using reflection, rotoinversion, and translation symmetry. Symmetry (Basel) 11:1132. https://doi.org/10.3390/sym11091132

29. Dreizen S, Snodgrasse RM, Webb Peploe H, Parker GS, Spies TD (1957) Bilateral Symmetry of Skeletal Maturation in the Human Hand and Wrist. AMA J Dis Child 93:122–127. https://doi.org/10.1001/archpedi.1957.02060040124004

30. Tümer N, Arbabi V, Gielis WP, de Jong PA, Weinans H, Tuijthof GJM, Zadpoor AA (2019) Three-dimensional analysis of shape variations and symmetry of the fibula, tibia, calcaneus and talus. J Anat 234:132–144. https://doi.org/10.1111/joa.12900

31. Stevens BW, Dolan CM, Anderson JG, Bukrey CD (2007) Custom talar prosthesis after open talar extrusion in a pediatric patient. Foot Ankle Int 28:933–938. https://doi.org/10.3113/FAI.2007.0933

32. Taniguchi A, Takakura Y, Tanaka Y, Kurokawa H, Tomiwa K, Matsuda T, Kumai T, Sugimoto K (2015) An alumina ceramic total talar prosthesis for osteonecrosis of the talus. J Bone Jt Surg - Am Vol 97:1348–1353. https://doi.org/10.2106/JBJS.N.01272

33. Tonogai I, Hamada D, Yamasaki Y, Wada K, Takasago T, Tsutsui T, Goto T, Sairyo K (2017) Custom-Made Alumina Ceramic Total Talar Prosthesis for Idiopathic Aseptic Necrosis of the Talus: Report of Two Cases. Case Rep Orthop. https://doi.org/10.1155/2017/8290804

34. Wang D, Wang Y, Wu S, Lin H, Yang Y, Fan S, Gu C, Wang J, Song C (2017) Customized a Ti6Al4V bone plate for complex pelvic fracture by selective laser melting. Materials (Basel) 10:. https://doi.org/10.3390/ma10010035

35. Boulay C, Tardieu C, Bénaim C, Hecquet J, Marty C, Prat-Pradal D, Legaye J, Duval-Beaupère G, Pélissier J (2006) Three-dimensional study of pelvic asymmetry on anatomical specimens and its clinical perspectives. J Anat 208:21–33. https://doi.org/10.1111/j.1469-7580.2006.00513.x

36. Osterhoff G, Petersik A, Sprengel K, Pape HC (2019) Symmetry Matching of the Medial Acetabular Surface-A Quantitative Analysis in View of Patient-Specific Implants. J Orthop Trauma 33:e79–e83. https://doi.org/10.1097/BOT.0000000000001373

37. Hernandez D, Garimella R, Eltorai AEM, Daniels AH (2017) Computer-assisted orthopaedic surgery. Orthop Surg 9:152–158. https://doi.org/10.1111/os.12323

38. Schendel S, Hazan-Molina H, Rachmiel A, Aizenbud D (2012) The Future in Craniofacial Surgery: Computer-Assisted Planning. Rambam Maimonides Med J 3:e0012. https://doi.org/10.5041/rmmj.10079

39. Perlick L, Bäthis H, Perlick C, Lüring C, Tingart M, Grifka J (2005) Revision total knee arthroplasty: A comparison of postoperative leg alignment after computer-assisted implantation versus the conventional technique. Knee Surgery, Sport Traumatol Arthrosc

13:167–173. https://doi.org/10.1007/s00167-004-0507-7

40. Verstreken K, Van Cleynenbreugel J, Marchal G, Van Steenberghe D, Suetens P (1996) Computer-assisted planning of oral implant surgery: An approach using virtual reality. Stud Health Technol Inform 29:423–434. https://doi.org/10.3233/978-1-60750-873-1-423

41. Wang GY, Huang WJ, Song Q, Qin YT, Liang JF (2016) Computer-assisted virtual preoperative planning in orthopedic surgery for acetabular fractures based on actual computed tomography data. Comput Assist Surg 21:160–165. https://doi.org/10.1080/24699322.2016.1240235

42. Cimerman M, Kristan A (2007) Preoperative planning in pelvic and acetabular surgery: The value of advanced computerised planning modules. Injury 38:442–449. https://doi.org/10.1016/j.injury.2007.01.033

43. Hu Y, Li H, Qiao G, Liu H, Ji A, Ye F (2011) Computer-assisted virtual surgical procedure for acetabular fractures based on real CT data. Injury 42:1121–1124. https://doi.org/10.1016/j.injury.2011.01.014

44. Lee P, Lai J, Hu Y, Huang C, Tsai Y, Ueng W (2012) Virtual 3D Planning of Pelvic Fracture. 24:245–262. https://doi.org/10.1142/S101623721250007X

45. Boudissa M, Chabanas M, Oliveri H, Tonetti J (2015) Virtual fracture reduction of the acetabulum using a rigid body biomechanical model. Rev Chir Orthopédique Traumatol 101:S187. https://doi.org/10.1016/j.rcot.2015.09.119

46. Upex P, Jouffroy P, Riouallon G (2017) Application of 3D printing for treating fractures of both columns of the acetabulum: Benefit of pre-contouring plates on the mirrored healthy pelvis. Orthop Traumatol Surg Res 103:331–334. https://doi.org/10.1016/j.otsr.2016.11.021

47. Sarkalkan N, Weinans H, Zadpoor AA (2014) Statistical shape and appearance models of bones. Bone 60:129–140

48. Felson DT, Neogi T (2004) Osteoarthritis: Is It a Disease of Cartilage or of Bone? Arthritis Rheum. 50:341–344

49. Gregory JS, Waarsing JH, Day J, Pols HA, Reijman M, Weinans H, Aspden RM (2007)

Early identification of radiographic osteoarthritis of the hip using an active shape model to quantify changes in bone morphometric features: Can hip shape tell us anything about the progression of osteoarthritis? Arthritis Rheum 56:3634–3643. https://doi.org/10.1002/art.22982

50. Bryan R, Surya Mohan P, Hopkins A, Galloway F, Taylor M, Nair PB (2010) Statistical modelling of the whole human femur incorporating geometric and material properties. Med Eng Phys 32:57–65. https://doi.org/10.1016/j.medengphy.2009.10.008

51. Querol LB, Büchler P, Rueckert D, Nolte LP, González Ballester MÁ (2006) Statistical finite element model for bone shape and biomechanical properties. In: Lecture Notes in Computer Science (including subseries Lecture Notes in Artificial Intelligence and Lecture Notes in Bioinformatics). Springer Verlag, pp 405–411

52. Skadlubowicz P, Krol Z, Wrobel Z, Hefti F, Krieg A (2010) Reconstruction of the pelvic region based on the statistical shape modeling. Adv Intell Soft Comput 69:165–173. https://doi.org/10.1007/978-3-642-13105-9_17

53. Grammer K, Thornhill R (1994) Human (Homo sapiens) facial attractiveness and sexual selection: the role of symmetry and averageness. J Comp Psychol 108:233–42. https://doi.org/10.1037/0735-7036.108.3.233

54. Adams GJ, Simoni DM, Bordelon CB, Vick GW, Kimball KT, Insull W, Morrisett JD (2002) Bilateral symmetry of human carotid artery atherosclerosis. Stroke 33:2575–2580. https://doi.org/10.1161/01.STR.0000035736.30488.7A

55. Vignesh U, Mehrotra D, Dichen, Anand V, Howlader D (2017) Three dimensional reconstruction of late post traumatic orbital wall defects by customized implants using CAD-CAM, 3D stereolithographic models: A case report. J Oral Biol Craniofacial Res 7:212–218. https://doi.org/10.1016/j.jobcr.2017.09.004

56. Stocks GW, Gabel GT, Noble PC, Hanson GW, Tullos HS (1991) Anterior and posterior internal fixation of vertical shear fractures of the pelvis. J Orthop Res 9:237–245. https://doi.org/10.1002/jor.1100090212

57. Mehra M, Somohano T, Choi M (2016) Mandibular fibular graft reconstruction with

CAD/CAM technology: A clinical report and literature review. J Prosthet Dent 115:123–128. https://doi.org/10.1016/j.prosdent.2015.05.012

58. Dell'Aversana Orabona G, Abbate V, Maglitto F, Bonavolontà P, Salzano G, Romano A, Reccia A, Committeri U, Iaconetta G, Califano L (2018) Low-cost, self-made CAD/CAM-guiding system for mandibular reconstruction. Surg Oncol 27:200–207. https://doi.org/10.1016/j.suronc.2018.03.007

59. Jansen J, Dubois L, Schreurs R, Gooris PJJ, Maal TJJ, Beenen LF, Becking AG (2018) Should Virtual Mirroring Be Used in the Preoperative Planning of an Orbital Reconstruction? J Oral Maxillofac Surg 76:380–387. https://doi.org/10.1016/j.joms.2017.09.018

60. Zhao H, Herman B, Adeeb S, Sheps D, El-Rich M (2013) Investigation of the geometries of the coronoid process and the fibular allograft as a potential surgical replacement. Clin Biomech 28:626–634. https://doi.org/10.1016/j.clinbiomech.2013.05.004

61. Komeili A, Westover LM, Parent EC, Moreau M, El-Rich M, Adeeb S (2014) Surface topography asymmetry maps categorizing external deformity in scoliosis. Spine J 14:973-983.e2. https://doi.org/10.1016/j.spinee.2013.09.032

62. Moody ML, Koeneman J, Hettinger E, Karpman RR (1992) The effects of fibular and talar displacement on joint contact areas about the ankle. Orthop Rev 21:741–4

63. Pahuta MA, Schemitsch EH, Backstein D, Papp S, Gofton W (2012) Virtual fracture carving improves understanding of a complex fracture: A randomized controlled study. J Bone Jt Surg - Ser A 94:1–7. https://doi.org/10.2106/JBJS.K.00996

64. Oliveri H, Boudissa M, Tonetti J, Chabanas M (2017) Planning acetabular fracture reduction using patient-specific multibody simulation of the hip. Med Imaging 2017 Image-Guided Proced Robot Interv Model 10135:101352P. https://doi.org/10.1117/12.2250380

65. Shen F, Chen B, Guo Q, Qi Y, Shen Y (2013) Augmented reality patient-specific reconstruction plate design for pelvic and acetabular fracture surgery. Int J Comput Assist Radiol Surg 8:169–179. https://doi.org/10.1007/s11548-012-0775-5

66. Ead MS, Duke KK, Jaremko JL, Westover L (2020) Investigation of pelvic symmetry using

CAD software. Med Biol Eng Comput 58:75–82. https://doi.org/10.1007/s11517-019-02068-w

67. Wong JML, Bucknill A (2017) Fractures of the pelvic ring. Injury 48:795–802. https://doi.org/10.1016/j.injury.2013.11.021

68. Yoshihara H, Yoneoka D (2014) Demographic epidemiology of unstable pelvic fracture in the United States from 2000 to 2009: Trends and in-hospital mortality. J Trauma Acute Care Surg 76:380–385. https://doi.org/10.1097/TA.0b013e3182ab0cde

69. Bjurlin MA, Fantus RJ, Mellett MM, Goble SM (2009) Genitourinary injuries in pelvic fracture morbidity and mortality using the national trauma data bank. J Trauma - Inj Infect Crit Care 67:1033–1039. https://doi.org/10.1097/TA.0b013e3181bb8d6c

70. Durkin A, Sagi HC, Durham R, Flint L (2006) Contemporary management of pelvic fractures. Am. J. Surg. 192:211–223

71. Flint L, Cryer HG (2010) Pelvic fracture: The last 50 years. J. Trauma - Inj. Infect. Crit. Care 69:483–488

72. Rothenberger DA, Fischer RP, Strate RG, Velasco R, Perry JF (1978) The mortality associated with pelvic fractures. Surgery 84:356–61

73. Sathy AK, Starr AJ, Smith WR, Elliott A, Agudelo J, Reinert CM, Minei JP (2009) The effect of pelvic fracture on mortality after trauma: An analysis of 63,000 trauma patients. J Bone Jt Surg - Ser A 91:2803–2810. https://doi.org/10.2106/JBJS.H.00598

74. Fotouhi J, Unberath M, Taylor G, Farashahi AG, Bier B, Taylor RH, Osgood GM, Armand M, Navab N (2018) Exploiting Partial Structural Symmetry for Patient-Specific Image Augmentation in Trauma Interventions. In: Lecture Notes in Computer Science (including subseries Lecture Notes in Artificial Intelligence and Lecture Notes in Bioinformatics). Springer Verlag, pp 107–115

75. Ead MS, Westover L, Polege S, McClelland S, Jaremko JL, Duke KK (2020) Virtual reconstruction of unilateral pelvic fractures by using pelvic symmetry. Int J Comput Assist Radiol Surg 15:1267–1277. https://doi.org/10.1007/s11548-020-02140-z

76. Borotikar B, Mutsvangwa T, Burdin V, Ghorbel E, Lempereur M, Brochard S, Stindel E,

Roux C (2017) Augmented statistical shape modeling for orthopedic surgery and rehabilitation. In: Medical Image Analysis and Informatics: Computer-Aided Diagnosis and Therapy. CRC Press, pp 369–425

77. Yokota F, Okada T, Takao M, Sugano N, Tada Y, Tomiyama N, Sato Y (2013) Automated CT segmentation of diseased hip using hierarchical and conditional statistical shape models. In: Lecture Notes in Computer Science (including subseries Lecture Notes in Artificial Intelligence and Lecture Notes in Bioinformatics). Springer, Berlin, Heidelberg, pp 190–197

78. Seim H, Kainmueller D, Heller M, Lamecker H, Zachow S, Hege HC (2008) Automatic segmentation of the pelvic bones from CT data based on a statistical shape model. In: EG VCBM 2008 - Eurographics Workshop on Visual Computing for Biomedicine. pp 93–100

79. Meller S, Kalender WA (2004) Building a statistical shape model of the pelvis. Int Congr Ser 1268:561–566. https://doi.org/10.1016/j.ics.2004.03.295

80. Chintalapani G, Ellingsen LM, Sadowsky O, Prince JL, Taylor RH (2007) Statistical atlases of bone anatomy: Construction, iterative improvement and validation. In: Lecture Notes in Computer Science (including subseries Lecture Notes in Artificial Intelligence and Lecture Notes in Bioinformatics). Springer, Berlin, Heidelberg, pp 499–506

81. Schutz H, Donovan ER, Hayes JP (2009) Effects of parity on pelvic size and shape dimorphism in Mus. J Morphol 270:834–842. https://doi.org/10.1002/jmor.10723

82. Fischer B, Mitteroecker P (2017) Allometry and Sexual Dimorphism in the Human Pelvis. Anat Rec 300:698–705. https://doi.org/10.1002/ar.23549

83. Van de Giessen M, Vos FM, Grimbergen CA, van Vliet LJ, Streekstra GJ (2012) An efficient and robust algorithm for parallel groupwise registration of bone surfaces. In: Lecture Notes in Computer Science (including subseries Lecture Notes in Artificial Intelligence and Lecture Notes in Bioinformatics). Springer Verlag, pp 164–171

84. Myronenko A, Song X (2010) Point set registration: Coherent point drifts. IEEE Trans Pattern Anal Mach Intell 32:2262–2275. https://doi.org/10.1109/TPAMI.2010.46

85. Betti L (2017) Human Variation in Pelvic Shape and the Effects of Climate and Past

Population History. Anat Rec 300:687–697. https://doi.org/10.1002/ar.23542

86. Turner W (1886) the Index of the Pelvic Brim As a Basis of Clasivicaiton. Am J Med Sci 181:252–253. https://doi.org/10.1097/00000441-188601000-00036

87. Caldwell WE, Moloy HC (1938) Anatomical Variations in the Female Pelvis: Their Classification and Obstetrical Significance. Proc R Soc Med 32:1–30. https://doi.org/10.1177/003591573803200101